uOttawa

L'Université canadienne
Canada's university

FACULTÉ DES ÉTUDES SUPÉRIEURES ET POSTOCTORALES

uOttawa

L'Université canadienne
Canada's university

FACULTY OF GRADUATE AND POSDOCTORAL STUDIES

Philippe Marchand
AUTEUR DE LA THÈSE / AUTHOR OF THESIS

M.A.Sc. (Electrical and Computer Engineering)
GRADE / DEGREE

School of Information Technology and Engineering
FACULTÉ, ÉCOLE, DÉPARTEMENT / FACULTY, SCHOOL, DEPARTMENT

Sequential Detection physical Network Coding in the Presence of Phase Asynchrony

TITRE DE LA THÈSE / TITLE OF THESIS

Abbas Yangaooglu
DIRECTEUR (DIRECTRICE) DE LA THÈSE / THESIS SUPERVISOR

CO-DIRECTEUR (CO-DIRECTRICE) DE LA THÈSE / THESIS CO-SUPERVISOR

M. El-Tanany

Claude D'Amour

Gary W. Slater
Le Doyen de la Faculté des études supérieures et postdoctorales / Dean of the Faculty of Graduate and Postdoctoral Studies

Sequential Detection of Physical Network Coding in the Presence of Phase Asynchrony

by

Philippe Marchand

Thesis Submitted to the
Faculty of Graduate and Postdoctoral Studies
In Partial Fulfillment of the requirements
For the M.A.Sc. Degree in Electrical and Computer Engineering

School of Information Technology and Engineering
Faculty of Engineering
University of Ottawa

Your file Votre référence
ISBN: 978-0-494-74194-8
Our file Notre référence
ISBN: 978-0-494-74194-8

Abstract

Physical-Layer Network Coding has the potential to greatly increase the throughput of wireless networks. This novel method of operating networks is based on the coherent demodulation of signals containing two waveforms transmitted synchronously. In this thesis, we explore the problems imposed by the physical constraints, in particular the carrier phase offset of the two signals making up the physical network code (PNC). For QPSK transmissions, coherent demodulation of the resulting symbols will be penalized by a decreased minimum distance resulting from carrier phase misalignment.

Based on the observation that binary signalling is not affected by this asynchrony, we propose a modulation framework which enables the coherent demodulation of PNC symbols with arbitrary phase offsets. The framework is based on bit-offset modulation by the sources and Maximum-Likelihood Sequence Detection by the receiver. The spread in receiver performance for a range of phase offset PNC signals is less than 2dB at moderate SNR for transmissions at a rate of 2 bits/symbol. These results confirm that the proposed solution is able to solve the problem of phase asynchrony for PNC QPSK and higher order modulations.

A mon épouse, Tracy, pour sa gentillesse et pour son support qui ont rendu cette thèse possible!

List of Abbreviations

AF	Amplify and Forward
ANC	Analog Network Coding
AWGN	Additive White Gaussian Noise
BPSK	Binary Phase Shift Keying
BER	Bit-Error Rate
DF	Decode and Forward
DNC	Digital Network Coding
EM	ElectroMagnetic
MLSD	Maximum-Likelihood Sequence Detection
MSK	Minimum Shift Keying
OQPSK	Offset Quadrature Phase Shift Keying
PNC	Physical-Layer Network Coding
QAM	Quadrature Amplitude Modulation
QPSK	Quadrature Phase Shift Keying
SNR	Signal to Noise Ratio
VA	Viterbi Algorithm

List of Symbols

a	Transmitted Data
c	Receiver-Generated Oscillator Signals
C	Capacity
d	Minimum Distance
E	Ending State
f_c	Carrier Frequency
$f()$	State Number Function
$g()$	Network Coding Mapping Function
k	Trellis State Index
M	Number of Signal Constellation Points
$M()$	Modulating Function
n	Discrete Time Index
r	Received Signal
s	Transmitted Passband Signal
S	Starting State
t	Continuous Time Index
T_b	Bit Duration
T_s	Symbol Duration
X	Transmitted Value
y	Transmitted Baseband Signal

Y	Received Value
z	Additive White Gaussian Noise
α	Preprocessed Transmit Sequence
β	Relay Amplification Factor
$\Gamma()$	OQPSK Modulation Term
θ	Carrier Phase
λ	Cumulative Metric
Λ	Set of Starting States
μ	Branch Metric
ξ_b	Bit Energy
Σ	Set of Ending States
ϕ	OQPSK Phase Modulation Term
Ψ	Amplitude Modulation Term
Ω	Amplitude

List of Figures

2.1 Butterfly Network using Traditional Routing 7
2.2 Butterfly Network using Network Coding 8
2.3 Canonical 2-way relay network 10
2.4 Earth-station and sattellite network 11
2.5 2-way relay network using traditional routing 11
2.6 Digital Network Coding applied to the 2-way relay network 12
2.7 Physical Network Coding applied to the 2-way relay network. 13
2.8 Analog Network Coding applied to the 2-way relay network. 15
2.9 Link capacities of the 2-way relay network 15
2.10 Capacity bounds for the different schemes applied to the 2-way relay network 19

3.1 2 Senders synchronously transmitting to a receiver 23
3.2 Signal space constellation with symbol mapping 24
3.3 PNC constellation for $M = 4$ 27
3.4 Constellation diagrams of the 2 source's BPSK signals and the resulting PNC signal 29
3.5 Normalized minimum distance of PNC constellations. 33

4.1 OQPSK constellation 36
4.2 OQPSK trellis representation 38
4.3 Trellis state progressions for PNC OQPSK: in-phase transitions 40
4.4 Trellis state progressions for PNC OQPSK: quadrature transitions 41

4.5 PNC constellation corresponding to Set 1 of the in-phase transition 42
4.6 8QAM constellation 45

5.1 PNC detection of BPSK: BER vs offset angle for different values of SNR ($\frac{\xi_b}{N_0}$) in dB 48
5.2 PNC detection of QPSK: BER vs offset angle for different values of SNR ($\frac{\xi_b}{N_0}$) in dB 50
5.3 Decoder performance of the MLSD of OQPSK for different values of $\theta_\triangle$ . . 51
5.4 MLSD of bit-offset OQPSK: BER as a function of $\theta_\triangle$ for different values of SNR ($\frac{\xi_b}{N_0}$) in dB 52
5.5 Probability of bit error for the MLSD of PNC 8QAM 55

List of Tables

5.1 Distance values of the error phases 54

Contents

Abstract i

List of Abbreviations iii

List of Symbols iv

List of Figures vii

List of Tables viii

1 Introduction 1

2 Theoretical Background 4

2.1 Wireless Communications 4

2.2 Network Coding 6

2.3 Digital Network Coding 9

2.4 Canonical 2-Way Relay Network 10

2.5 Physical Network Coding 12

2.6 Analog Network Coding 14

2.7 Capacity Analysis 15

2.7.1 Traditional Routing Capacity 15

2.7.2 DNC Capacity 16

2.7.3 ANC Capacity 16

2.7.4 PNC Capacity 18

3 Asynchrony and PNC Systems **20**

3.1 Synchronization Assumption 20

3.2 System Model 23

3.3 Symbol Ambiguity 26

3.4 Minimum Distance 32

4 MLSD of bit-Offset PNC **34**

4.1 Offset Quadrature Phase Shift Keying 35

4.2 Physical Network Coded OQPSK 37

4.3 Trellis Representation of PNC signals 39

4.4 Generalization of the MLSD 43

5 Performance Evaluation **47**

5.1 Regular Detection of BPSK PNC 48

5.2 Regular Detection of QPSK PNC 49

5.3 Proposed Solution Results: OQPSK PNC 50

5.4 Error Bounds on the MLSD of PNC 53

5.5 MLSD of Offset 8QAM PNC 55

6 Conclusion **57**

6.1 Contributions 57

6.1.1 Problem Statement 57

6.1.2 Proposed Framework Solution 58

6.2 Future Research 59

Bibliography **61**

Chapter 1

Introduction

In an attempt to maximize network throughput to accommodate the plethora of new communication systems that are continually developed, network coding has been proposed as a new method for transmitting information through multiple nodes. The main idea behind network coding is to allow intermediate network nodes to mix independent signals as they progress from a source to a destination. This contrasts with traditional routing used in current systems, where information streams are kept separate and assigned to distinct channels as they make their way through the network. With network coding, a destination is able to leverage its knowledge of the higher layers of communication to undo the mixing and recover its intended information. The concept was originally proposed by Ahlswede *et al.*, who showed that coding was necessary to achieve the min-cut max-flow bound of a network [1]. Subsequently, considerable research has been ongoing to develop systems which benefit from applying this new way of operating networks.

One such effort is the porting of network coding to wireless networks. This medium is a particularly good setting in which to apply network coding as its broadcast nature ensures a greater receptivity of emitted signals and more opportunities to combine different information streams. Two systems, which apply coding at different levels, have been proposed: the first system performs the mixing at the digital level, requiring a relay node to decode both streams and then combine the resulting digital symbols to make the network

coded symbols. Researchers have developed real-life systems that utilize digital network coding, and in particular, the COPE architecture, which XORs bits from two different packets to form a network coded stream, has been applied to wireless mesh networks to provide marked throughput gains [2]. The second system goes one step further and lets the physical media mix the signals, in effect exploiting the additive interference that results when two waveforms are transmitted simultaneously. Physical-layer Network Coding lets two sources broadcast at the same time and has the destination demodulate the resulting signal to obtain the symbolic addition of the two sources' original data [3]. More concurrency is possible with PNC, which leads to even more impressive gains than are possible with digital network coding (DNC). Unfortunately, PNC is still a theoretical proposal which has unrealistic physical layer assumptions. To circumvent these limitations, researchers have developed Analog Network Coding (ANC), which exploits the inherent asynchrony of the wireless media by using a non-coherent demodulation to recover the original symbols from a waveform containing interference from two sources [4]. Although enticing theoretical throughput gains are again demonstrated, this scheme in fact suffers from a degraded capacity resulting from its inability to fully combine signals. To address the problems arising from the limitations of these two network coding systems which mix at the physical layer, we propose a receiver signal processing algorithm which allows for the coherent reception of PNC signals under more realistic physical-layer scenarios.

The contribution of this thesis is a modulation and demodulation framework that enables the coherent decoding of PNC signals. We propose a Maximum Likelihood Sequence Detection (MLSD) algorithm to extract two sources' joint information from a received signal made up of the addition of both sources' waveforms. This signal detection algorithm is able to overcome the problem of carrier phase misalignment, the most probable asynchrony in wireless network coding systems employing mixing at the physical layer. By foregoing the restrictions of the physical network coding systems proposed so far, the proposed framework is general enough to allow for the development of new systems. This thesis is organized as follows: Chapter 2 reviews the current state of the art of wireless communications and network coding. Chapter 3 focuses on the issues involved in receiving

signals mixed at the physical layer, with a close attention on the problems of asynchrony. Chapter 4 introduces the MLSD of physically-mixed, bit-offset modulated signals. Finally, Chapter 5 presents the performance evaluation of the proposed framework.

Chapter 2

Theoretical Background

In this section, we present a review of wireless communications and examine the progress made in the area of network coding, with a focus on the current systems proposed in the literature.

2.1 Wireless Communications

Recently, there has been an increased focus on multi-user communication and a shift towards designing networks by considering their aggregate collection of links [5]. Communication networks were traditionally understood as a collection of independent point-to-point links which were developed and optimized separately to form a working system. When this single-user approach is taken to designing wireless networks, nodes are in direct competition with their neighbours for throughput. Indeed, the broadcast nature of the medium results in varying levels of interference for anyone who is not the intended receiver of a node's transmission. In contrast, multi-user communications takes a more holistic approach to network design by jointly developing the links making up the system. It is able to leverage a node's knowledge of the higher layers of communications to circumvent interference and achieve a more efficient operation.

Multi-user network design research has been motivated by the work of Gupta and

Kumar, who proved that in a traditional single-user environment, a user's throughput capacity is inversely proportional to the number of terminals in a network [6]. In this work, the authors attempt to quantify, in an information theoretic sense, the transport capacity of general networks made up of nodes seeking to transmit to randomly selected destinations. They consider multihop transmission, with which a source's packets are relayed by intermediate nodes until they reach their destinations. A packet is received successfully if either the Protocol or Physical Model constraints are met. Both models correspond to traditional single-user communication since a destination experiences complete interference from transmissions for which it is not the intended receiver. The result of this general study prove that the transmission capacity of a terminal connecting to an Ad-Hoc network with n nodes is bounded by $O(\frac{1}{\sqrt{n}logn})$. This conclusion implies that the throughput available to a source will degrade to zero as the network to which it connects acquires a greater density of users. Essentially, it is the need for the nodes to share space and the transmission medium which limits their throughput. This conclusion offers a pessimistic outlook on the scalability of single-user wireless communication systems and underscores the challenges involved in building large networks. Clearly, multi-user strategies will be needed to overcome these limitations.

Things are not completely hopeless, however, as recent work has shown that we can extricate better performance from wireless networks by using multi-user strategies. For example, Gupta and Kumar have revealed that it is possible for a certain class of networks to achieve a transport capacity that scales with the number of terminals [7]. This was accomplished by letting nodes use an interference cancellation algorithm to relay information to the intended destinations. Using a different approach, the work of Laneman *et al.* validates the use of relays to overcome channel outages brought about by multipath fading [8, 9]. In this work, principles developed for multi-antennae systems were adapted to relay networks and protocols were designed to leverage cooperative diversity in a multi-node network. Results show that interesting power savings are possible for a given transmission reliability when using redundant transmission paths to reach a destination.

2.2 Network Coding

Of course, network coding is another multi-user strategy that offers hope of realizing wireless networks which support an increased number of users. Network coding has been shown necessary in achieving the transmission capacity of certain classes of networks [1]. The authors have shown that the multicast capacity of a network, defined as the maximum rate at which a sender can transmit common information to a set of receivers, is possible with network coding. This multicast capacity is in turn equal to the min-cut max-flow rate, which is given by the flow through the minimum cut of the network separating the sender from any receiver [10]. Interestingly, the multicast capacity rate was shown impossible when using traditional routing [1]. Network coding is therefore an interesting tool for network designers in their attempt to build systems which have a large number of users with access to an appreciable amount of bandwidth.

The basic concept of network coding has been succinctly explained with the use of the example shown in Figure 2.1[1]. In this so-called Butterfly Network, one sender attempts to multicast to two destinations with the help of 4 relay nodes connected by unity capacity links. This network represents a wired environment, as the links are completely independent. By applying the min-cut max-flow theorem, it is straightforward to see that the maximum rate at which the sender can multicast to the two destinations is 2 information blocks to the 2 receivers at every time instant. Referring to Figure 2.1, sender S has two information blocks, X_1 and X_2, to multicast to the two destinations, *T1* and *T2*. We assume instantaneous reception and retransmission at the intermediate nodes and indicate the information block relayed on each link at the given time instant. As seen on Figure 2.1, capacity rate multicast of these two information units is impossible with traditional routing, as relay $R3$ will have to alternate between forwarding the information incoming on both its edges. It puts X_1 on the link connecting it to $R4$ during the first time instant, t_1. During the second instant, t_2, it instead forwards the X_2 value. The two blocks of information will therefore take *two* time instants to reach the two destinations.

The key insight of the authors was to realize that information is modifiable as it

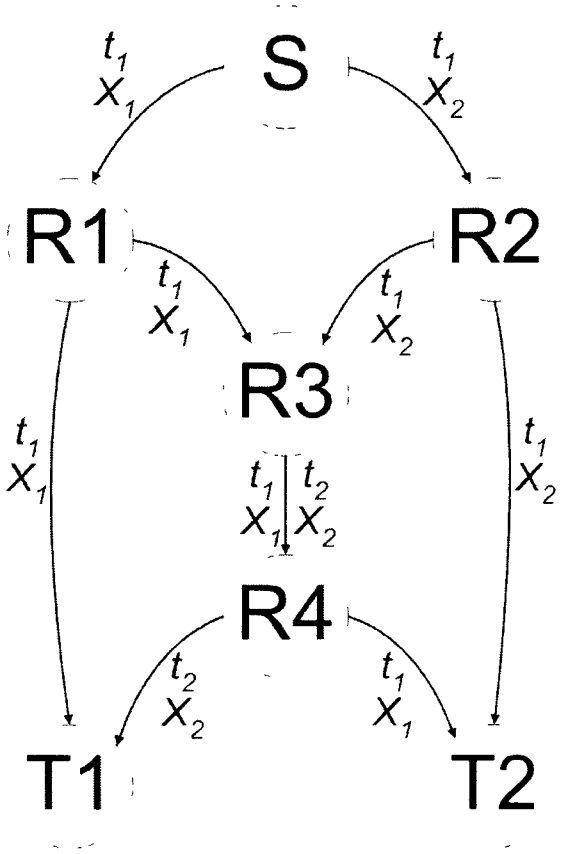

Figure 2.1: Butterfly Network using Traditional Routing

progresses through a network and that links can be shared by different information blocks [1]. In the Butterfly Network example, $R3$ can combine both information blocks and forward that on instead. As seen in Figure 2.2, this node now transmits a mixed version X_1 and X_2. The time index of each link transmission is not displayed as the multicast exhange is carried out in a single instant. The destinations can use the block of information they received unmodified to reverse the mixing and recover the other information block. Thus, by letting intermediate nodes combine different information streams, the multicast capacity rate of 2 information units to the 2 sources at each time instant is possible.

Starting from this initial proposal, network coding has garnered considerable attention. Various approaches were taken to establish and generalize the concept. Interesting results were derived for wired networks, to which network coding was originally adapted. Li and

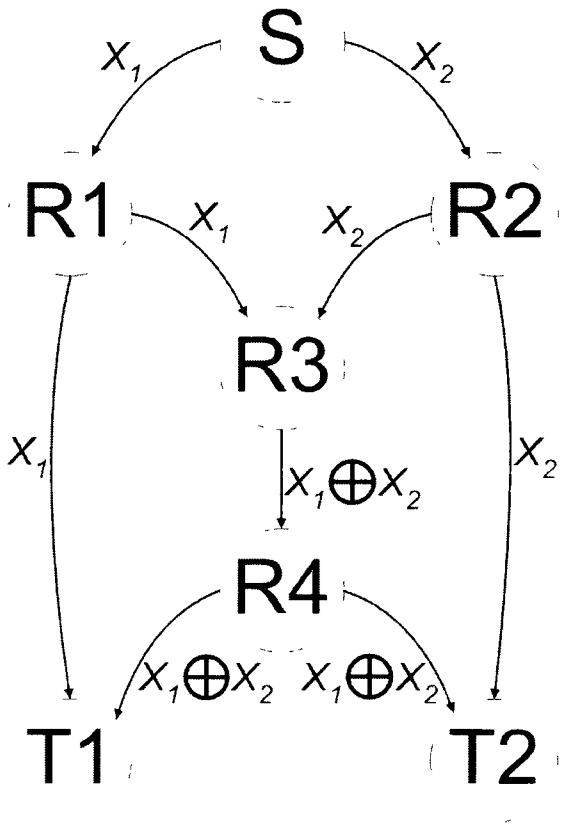

Figure 2.2: Butterfly Network using Network Coding

Yeung have shown that linear codes are sufficient in achieving the capacity of multicast networks [11]. Koetter and Médard then provided an algebraic framework for the analysis of these linear network codes [12]. In their work, the network uses a Galois Field over which relay nodes apply the linear combination of symbols. Receiver nodes, which have knowledge of the network's effect on their received data, are able to reverse the mixing operations and recover the original data. A random operation of networks was shown possible by having the relay nodes mix symbols using arbitrary linear combinations [13]. The authors show that a destination is able to recover its intended information with high probability given a large field size. Thus, network coding has the added benefit of enabling a decentralized and random network operation.

Porting network coding to a wireless environment has been initiated by the work of Lun

et al. [14]. In this work, wireless links are modelled as being broadcast and experiencing attenuation, as well as incurring a cost reflective of the power or delay necessary for transmission. The benefits of network coding are leveraged to obtain, in a decentralized manner, minimum-cost multicast connections in coded packet networks [14].

Research has also been carried out to develop practical systems which could benefit from these theoretical findings. This work required a selection of the actual information units on which to base network codes. In their original proposal, Ahlswede *et al.* leave the network coding concept in a general state. The notion of coding flow units as they make their way through a network could be applied to various information elements, from simple analog signals to abstract discrete symbols. Indeed, network coding's only requirement is that the mixing carried out by the intermediate nodes be reversible [1]. Many types of network data could apply to the information symbols of the algebraic framework proposed in [12].

2.3 Digital Network Coding

The development of practical systems benefited from the work of Katti *et al.* [2, 15], who chose to apply network codes at the packet level. In their proposed COPE architecture, network terminals XOR the individual bits of the different packets they have to transmit. Their system works in the following way: at one time instant, a node may have n packets in its queue to transmit. To carry out network coding, it mixes the n packets and broadcast the resulting combination to its neighbours. The receivers, who have knowledge of at least $n-1$ of the combined packets, are able to undo the mixing and recover the packet which they were missing. The system is restricted by the need of the receivers to have copies of all but one of the packets making up the network coded packet. Nevertheless, network terminals are able to keep track of the contents of their neighbours' buffers and transmit the correct combination of packets. A wireless mesh network testbed was able to realize interesting throughput gains [15, 16].

2.4 Canonical 2-Way Relay Network

The authors note that the maximum asymptotic coding gain of their systems is 2, which occurs in the idealized setting where an infinite series of nodes arranged linearly relay packets for two end terminals [15]. A suboptimal subset of this network is shown in Figure 2.3. In this canonical two-way wireless network, two sources, which are out of range, attempt to exchange packets with the help of a relay. Senders $S1$ and $S2$ have packets X_1 and X_2 to transmit, respectively, and must receive the other's packets.

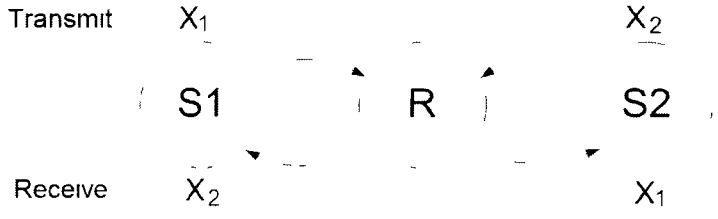

Figure 2.3: Canonical 2-way relay network

This configuration has been studied in a non-network coding setting [17, 18] and serves as a good benchmark with which to evaluate the proposed systems. Two-way information exchanges are a basic building block of many networks and are seen in numerous real-life applications. The canonical two-way network not only applies to cases where two end terminals exchange information, such as when cellular telephones communicate by transmitting through a base station. It also models many core network transmissions involving bidirectional flows [19], for example the earth-station and satellite network seen in Figure 2.4. In this situation, information streams which must travel large distances are transmitted by an earth station to a satellite. The satellite acts as a relay and retransmits back to earth, in effect connecting the two stations. As there are information flows in both directions, the stations are assigned orthogonal channels on which to transmit and receive.

As the canonical 2-way relay network is used in many real-life settings, increasing

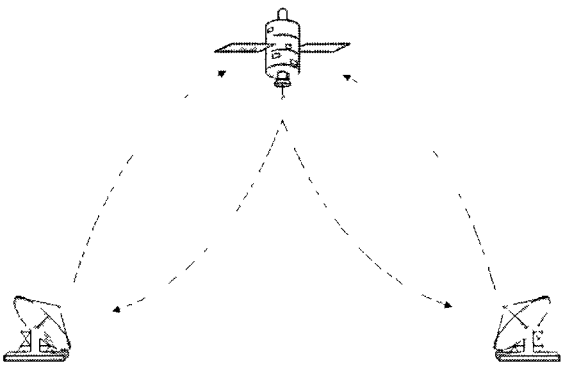

Figure 2.4: Earth-station and sattellite network

its capacity will have widespread benefits. There are several solutions to the problem of information exchange in the 2-way network, and as we shall see, all are of varying efficiency. The focus of the rest of the thesis on this network configuration.

In current systems, the two end points of the relay network divide up the available bandwidth. The operation of the 2-way relay network using traditional routing is illustrated in Figure 2.5. The 2 sources, $S1$ and $S2$, have information $X1$ and $X2$ to transmit, respectively and all exchanges are modulated with function $M()$. The four links in the network take their turn and the information exchange is carried out in four time instants.

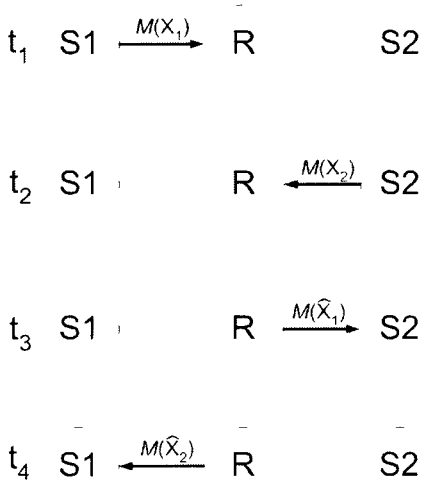

Figure 2.5: 2-way relay network using traditional routing

Returning our attention to COPE, the operation of the 2-way network is now represented in Figure 2.6. The two sources S_i, $i \in 1,2$ take turns transmiting information X_i, which relay R decodes to obtain $\hat{X}_i$. The relay then broadcasts the network coded combination to both sources, now acting as receivers. From this received network coded information, the two nodes are able to recover the other's information by reversing the mixing using their own data which they just transmitted. A total of 3 transmissions are taken for this exchange as opposed to the 4 that are necessary with traditional systems. As there are $n = 2$ links in this linear network, the coding gain is indeed $\frac{2n}{n+1} = 1.33$ [15].

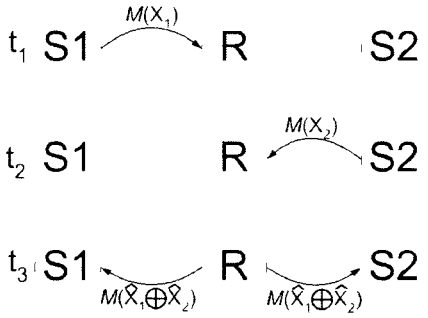

Figure 2.6: Digital Network Coding applied to the 2-way relay network

2.5 Physical Network Coding

Other work on building practical systems explored the concept of using network coding on fully analog signals. As electromagnetic (EM) waves interfere in an additive fashion, it could be possible to let the wireless medium perform the mixing. The authors of [3] propose Physical-layer Network Coding (PNC) to investigate this idea. This scheme works with two sources' simultaneous transmission and a receiver's demodulation of the resulting joint signal. This joint signal is created by the addition of the two waveforms and represents network coded information. It is mapped by the receiver to symbol values corresponding to the $GF(2^m)$ addition of the sources' original message data, where $M = 2^m$ is the number of points in the sources' constellations.

The PNC system was adapted to the two-way relay network. The high level representation of the PNC exchange is pictured in Figure 2.7. The two sources now transmit concurently in the first time instant, resulting in an interference signal which the relay demodulates to obtain an estimate of the joint data, $X_1 \hat{\oplus} X_2$. In the second time instant, a signal modulated by this joint data is broadcast to $S1$ and $S2$. The other source's information is recovered by undoing the mixing to complete the exchange.

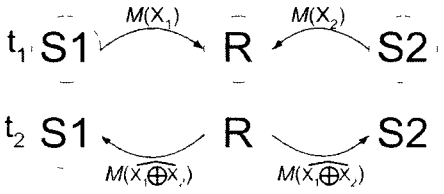

Figure 2.7: Physical Network Coding applied to the 2-way relay network.

The authors obtain bounds on the capacity of the 2-way relay network using PNC [3]. They break up the system into two components, a multiple-access link when the two sources are simultaneously transmitting to the relay and a regular single-source link when the relay broadcasts back to the sources, now acting as receivers. Of the two links, the former is unique to the PNC scheme and determines the overall performance of the two-way relay network. This link is not the traditional multiple-access link familiar to information theorists, however. In a traditional multiple-access link, the receiver must extract both sources' data from a received interference signal [20]. In a PNC multiple-access link, the receiver must instead obtain the *joint* information of the two sources from the interference signal [3]. The authors' analysis reveals that during this transmission, the PNC symbols possess the same minimum distance as the original signals of the sources [3]. They therefore conclude that the capacity of the multiple-access PNC link is similar to that of a single-access link. However, as only two time slots are necessary for the sources to exchange information, the overall capacity of two-way network using PNC is twice that of traditional transmission and 50% superior to the DNC scheme.

We will elaborate further on the physical constraints of this system and discuss the effects of asynchrony on the decoding of PNC symbols in the next chapter.

2.6 Analog Network Coding

Analog Network Coding (ANC) is the last system we consider [4]. In essence, this scheme combines the simultaneous transmission and EM wave mixing distinctive of PNC with the concept of Amplify-and-Forward (AF) relaying [17]. ANC uses a non-coherent detection that is immune to the asynchrony of the two sources. However, this scheme suffers from a degraded capacity resulting from redundant signalling.

This system is understood with the two-way relay network example, shown in Figure 2.8. The two sources again transmit concurrently to the relay node in the first time instant, which then broadcasts to both receivers in second instant. As opposed to the PNC scheme, however, the relay does not attempt to decode the mixed signal. Instead, it simply retransmits a copy of the interference signal made up of both sources' waveforms. During the second time instant, both sources receive this forwarded interference signal. Figure 2.8 shows this relayed interference signal made up of the two signal components from the 2 sources as well a Z term representing the AWGN at R. The interference is scaled by β, which we will describe in more detail in the next section.

The authors propose an architecture in which transmitters employ Minimum Shift Keying (MSK) signalling and receivers use a non-coherent reception enabled by the relative angle modulation of MSK. The receivers compute the phase change from the previous to the current received sample to obtain an estimate of the sources' joint data. This phase change represents 2 possible pairs of values corresponding to the two sources' messages. The receiver selects the pair in agreement with the message which it transmitted during the first time instant. The other source's message follows directly and is recovered to complete the exchange of information.

As with the PNC scheme, ANC completes the two-way relay exchange in two time periods and has a network coding throughput gain of 2. ANC has been ported to other networks, notably the extended relay chain and, interestingly, the X-topology network [4]. As discussed above, the former is an extension of the two-way relay network while the latter is inspired by the multicast Butterfly Network. We will next examine the capacity

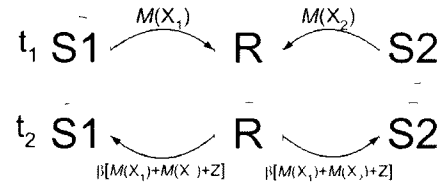

Figure 2.8: Analog Network Coding applied to the 2-way relay network.

of the 2-way relay network operating under the different network coding schemes.

2.7 Capacity Analysis

To get a clear grasp on the merits of the different network coding schemes, it is helpful to quantify the capacity of the 2-way relay network operating under the various proposed systems. We refer to Figure 2.9, which shows the channel capacities of the 4 links making up the canonical relay network.

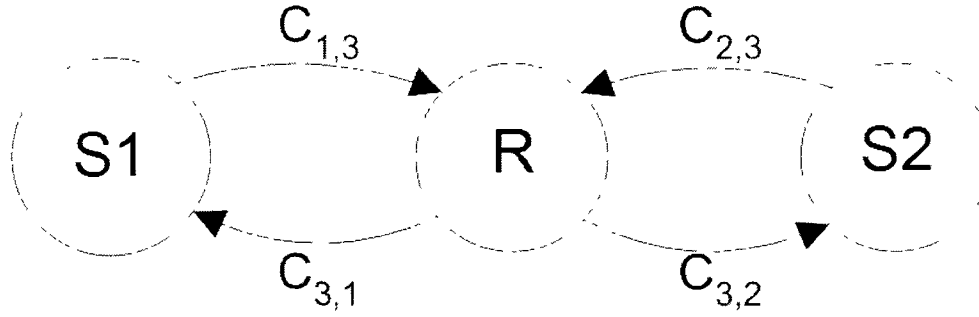

Figure 2.9: Link capacities of the 2-way relay network

2.7.1 Traditional Routing Capacity

The traditional routing scheme works by having the sources take turns transmitting. The relay receives, buffers and retransmits the two signals in separate transmissions. Therefore, the channel from one source to a receiver is equivalent to two successive Gaussian links and the overall capacity is constrained by the minimum capacity of the two. As each

channel is used for $\frac{1}{4}$ of the time, we get the following expression for the total transport capacity of the traditional routing scheme [4]:

$$C_{traditional} = \frac{1}{4}\min\{C_{1,3}, C_{3,2}\} + \frac{1}{4}\min\{C_{2,3}, C_{3,1}\} \tag{2.1}$$

where the capacity of a Gaussian link is given by

$$C_{i,j} = \log(1 + SNR_{i,j})$$

with $SNR_{i,j}$ the Signal to Noise Ratio (SNR) at the receiver end of the link connecting node i to node j. Assuming equivalent links, (2.1) reduces to

$$C_{traditional} = \frac{1}{2}C = \frac{1}{2}\log(1 + SNR) \tag{2.2}$$

2.7.2 DNC Capacity

DNC is the next scheme which was proposed. We assume that the relay's broadcast to both $S1$ and $S2$ during the third time period can be treated in the same way as the single-destination links. Specifically, $C_{3,2} = C_{3,1} = C_3$. Therefore, the capacity of this scheme is given by

$$C_{DNC} = \frac{1}{3}\min\{C_{1,3}, C_3\} + \frac{1}{3}\min\{C_{2,3}, C_3\}$$

We again assume that all transmissions are identical, such that

$$C_{DNC} = \frac{2}{3}\log(1 + SNR) \tag{2.3}$$

Digital network coding is therefore $\frac{1}{3}$ times more efficient than traditional routing.

2.7.3 ANC Capacity

Even more efficiency is possible with ANC as the 2-way exchange is accomplished in only 2 time periods. However, this scheme is hampered by the relaying it employs on the combination signal. To obtain an expression for capacity, we let sources *S1* and *S2*

transmit values $X_1[n]$ and $X_2[n]$, respectively. In order to simplify analysis, we discard the channel gains present in the derivation of [21]. After *S1* and *S2* transmit concurrently, relay R receives value

$$Y_3[n] = X_1[n] + X_2[n] + Z_3[n]$$

where $Z_3[n]$ is the AWGN present at the receiver. To respect its power budget, R scales this value to obtain $X_3[n]$, the sample it transmits back to both sources:

$$X_3[n] = \beta Y_3[n]$$

where

$$\beta = \sqrt{\frac{SNR}{2SNR + 1}}$$

Receiver $S1$ will then receive signal

$$\begin{aligned} Y_1[n] &= X_3[n] + Z_1[n] \\ Y_1[n] &= \beta Y_3[n] + Z_1[n] \\ Y_1[n] &= \beta(X_1[n] + X_2[n] + Z_3[n]) + Z_1[n] \end{aligned} \tag{2.4}$$

where $Z_1[n]$ is the AWGN. $S1$ knows the message it transmitted in the first time instant, which it eliminates from (2.4). This yields

$$Y_1[n] = \beta X_2[n] + \beta Z_3[n] + Z_1[n] \tag{2.5}$$

which $S1$ uses to estimate $S2$'s data. The relay replicates the noise it received in the first time instant, which accounts for the 2 noise terms in (2.5). As the two receivers are symmetrical, the capacity of the 2-way relay network using ANC follows from (2.5) and is given by:

$$C_{ANC} = \log(1 + \frac{SNR^2}{3SNR + 1}) \tag{2.6}$$

This result highlights the weakness of the ANC scheme, which is not able to combine information in a network coding sense. Indeed, the relay must allocate half of its power budget to each signal component making up the ANC symbol. This is suboptimal, as the

intended receivers of the ANC symbol have knowledge of one of the two signal components. The relay expends energy to transmit information already known by the destinations.

This degradation in performance has been noticed previously [21]. Work has focused on operating ANC in the high SNR regime, where it is less vulnerable to noise propagation [22].

2.7.4 PNC Capacity

Decidedly, AF relaying incurs a performance penalty when used for network coding. In contrast, the PNC adopts a Decode and Forward (DF) [17] scheme which is able to better combine signals. The authors contend that the relay is able to decode PNC symbols at a Bit Error Rate (BER) similar to the single-signal case [3]. Thus, the PNC transmission by $S1$ and $S2$ to the relay is equivalent to a single-source link and we set $C_{1,3} = C_{2,3} = C_3$. We obtain the following expression for the capacity of the 2-way network using PNC:

$$C_{PNC} = \frac{1}{2}\min\{C_3, C_{3,1}\} + \frac{1}{2}\min\{C_3, C_{3,2}\}$$

and again assuming similar link capacities, we get

$$C_{PNC} = \log(1 + SNR) \tag{2.7}$$

PNC is therefore able to double the throughput of traditional routing. This result is in agreement with the putative potential of network coding, which makes it possible to add the flow capacities of separate signal transmissions through a network when multicasting [1].

Figure 2.10 shows a plot of the capacity of the 2-way network utilizing the different relaying strategies. The performance penalty incurred by ANC is noticeable at low SNR, where it is inferior to even traditional routing. Clearly, the DF relaying of PNC has the potential to deliver the highest troughput gains.

These results assume that the capacity of the PNC multiple-access link is similar to that of a regular single-source link. We will see in the next section that the physical constraints can lower the capacity of this link when used in the manner proposed in [3].

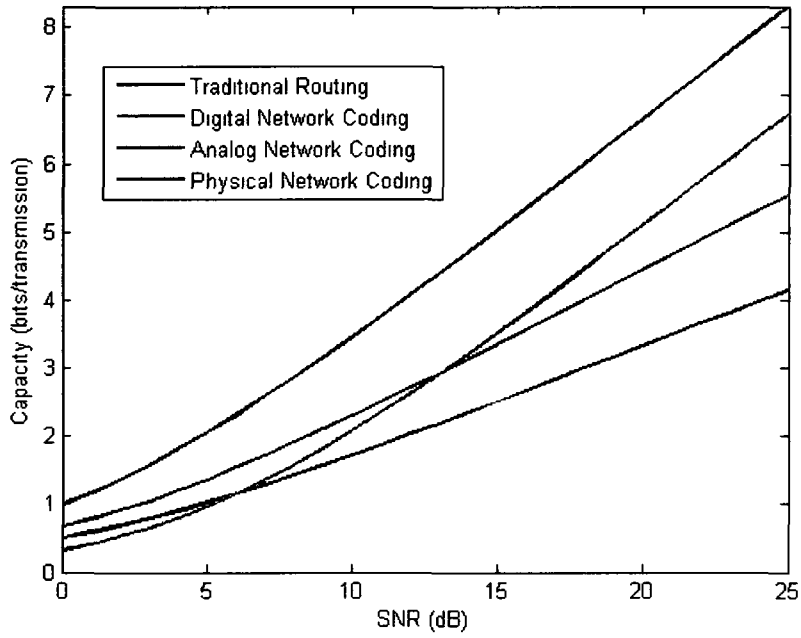

Figure 2.10: Capacity bounds for the different schemes applied to the 2-way relay network

In fact, foregoing the carrier synchronization assumption and allowing for arbitrary phase offsets will yield unworkable systems. What is needed is a joint decode of physically mixed signals that is immune to a lack of synchrony between the two sources.

Chapter 3

Asynchrony and PNC Systems

In this chapter, we establish an understanding of the outstanding issues that must be resolved before PNC systems can be deployed. In particular, we will explore the issues related to the synchronous reception of two signals, with a description of the steps necessary for the demodulation of PNC symbols and a quantification of the effect of carrier phase offset.

3.1 Synchronization Assumption

In essence, PNC systems work by demodulating interference signals. Naturally, there must be stringent synchronization requirements in getting independent waveforms to add constructively in mid-air. First off, all the symbols must be received at the same time. As the signals are wireless, their passband parameters must also be in agreement for them to combine properly and yield a PNC signal which can be demodulated. The synchronization of carrier frequency and phase will therefore also have an effect on the performance of PNC systems.

The authors of [3] analyze the effects of asynchrony of these 3 parameters for PNC symbols made up of BPSK signals. Their analysis reveals that a minimal performance penalty of 1 to 3 dB can be expected from the asynchrony of symbol timing, carrier

frequency or carrier phase. As these results apply only to BPSK modulation, we have a limited characterization of the effects of asynchrony on PNC systems. In the next section, we will explore the effects of phase asynchrony on PNC systems employing other modulation schemes. To justify our focus on carrier phase offset, we will now compare it to the other two asynchronies, carrier frequency and symbol timing.

The relative difficulty in synchronizing carrier phases stems from the lack of control over this parameter. The impracticality of PNC systems which seek to synchronize both their carriers' phases is best understood by considering the demanding requirements of such systems. First off, a PNC system which requires perfect phase alignment would need a way for one of the sources to adapt its carrier phase. In traditional single signal systems, no attempt is made at setting the carrier phase *a priori*. Instead, receivers are able to decode signals with an arbitrary phase by adapting their demodulation parameters. Thus, new transmitter hardware which dynamically alters the oscillator phase would have to be developed. This is a non-trivial undertaking, particularly if systems have a cost or size constraint.

Furthermore, as only the receiver is able to know the phase difference between the two carriers, the hypothetical PNC system would be required to relay this knowledge from the receiver back to one of the sources. While certainly feasible, this requirement would complicate the operation of the PNC system.

Finally, assuming that a source is able to obtain knowledge of the offset and adjust its carrier phase, it is still doubtful that the PNC receiver could receive two perfectly phase aligned signals for extended periods. The phase of a wave at a receiver is a function of not only the intrinsic phase of the oscillator at the transmitter but also of the channel from source to destination taken by the signal. Thus, the mobility of the nodes or time-varying channel effects would nullify any adjustments made by the system.

The scaling problem inherent in carrier phase control becomes noticeable when compared to the problem of symbol timing synchronization. For example, GSM wireless transmissions have a symbol rate that is in the range of 270KHz, an order of magnitude less than the carrier frequency, which is in the range of 900MHz. A synchronization mech-

anism which aligns the phases of two transmitters would need to be orders of magnitude more precise than a mechanism to adjust the symbol timing.

To illustrate the effects of this scale difference, consider a PNC system built using the GSM air interface. Assume that both sources are in perfect *intrinsic* synchrony: they are able to emit symbols at exactly the same time using carrier waves that are at precisely the same phase. However, one source is located a quarter of a wavelength, $\frac{\lambda}{4} = 7.5\text{cm}$, closer to the receiver than the other. The signals travel unequal distances and therefore arrive out of phase and with a symbol timing offset. The carrier phase offset represents $\frac{\pi}{2}$ radians, and as we will see in the next section, makes the demodulation of some phase modulated PNC symbols impossible. The resulting symbol timing offset, on the other hand, is easily compensated. Indeed, the time offset is only $\frac{7.5cm}{3\times10^8 m/s} = 0.5\text{ns}$ and represents a minute fraction of the symbol duration, which is in the range of the micro seconds.

Carrier frequency is also more easily synchronized than phase. Frequency is an absolute quantity that is more amenable to synchronization. A physical network coded system could have frequency specifications and tolerances, which transmitter manufacturers could then design for. The received carrier phase, on the other hand, is a relative value that is dependent on factors outside the control of the transmitter. There is no absolute phase value to aim for when designing a transmitter. Therefore, in the hierarchy of asynchronies which preclude the deployment of PNC systems, carrier phase must be put at the front. The other asynchronies will also have negative effects and are worth investigating, but the problem of phase asynchrony must be solved first. PNC systems will need to work with the current technological paradigm and assume arbitrary carrier phase offsets. We will see in the next section that the capacity of a PNC link can be severely degraded when there is a carrier phase misalignment.

3.2 System Model

We now shift our focus to the receiver of PNC signals seen Figure 3.1. Nodes $X1$ and $X2$ are synchronously emitting waveforms which add up in the vicinity of T. Receiver T attempts to decode the resulting interference signal and recover the PNC data.

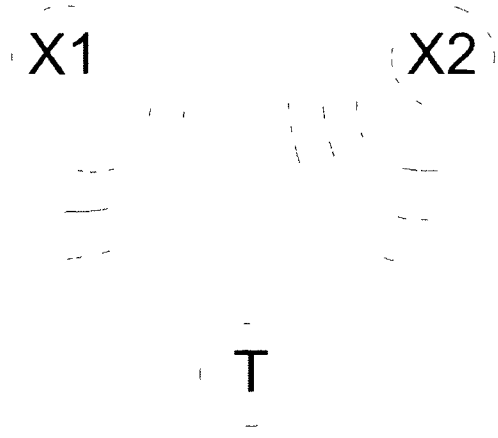

Figure 3.1: 2 Senders synchronously transmitting to a receiver

Nodes $X1$ and $X2$ transmit independent information $a_1, a_2 \in 0, 1, ...M-1$, respectively. The two transmitters use identical $M-$ary phase modulation and map their information to a complex baseband value using

$$y(a_i) = e^{\frac{j2\pi a_i}{M}} \tag{3.1}$$

Figure 3.2 illustrates this modulation for the case of $M = 4$.

The sources are transmitting equal energy phase modulated signals s_1 and s_2, respectively, given by

$$s_i(t, a_i) = Re\{y(a_i)\}\cos(2\pi f_c t + \theta_i) + Im\{y(a_i)\}\sin(2\pi f_c t + \theta_i) \quad for \quad 0 \leq t < T_s$$

where f_c is the carrier frequency and θ_i the intrinsic carrier phase of source i. As both sources transmit concurrently, the EM waves of both signals add up to give $r(t)$, the PNC signal received by R,

$$r(t, a_1, a_2) = s_1(t, a_1) + s_2(t, a_2) + z(t) \tag{3.2}$$

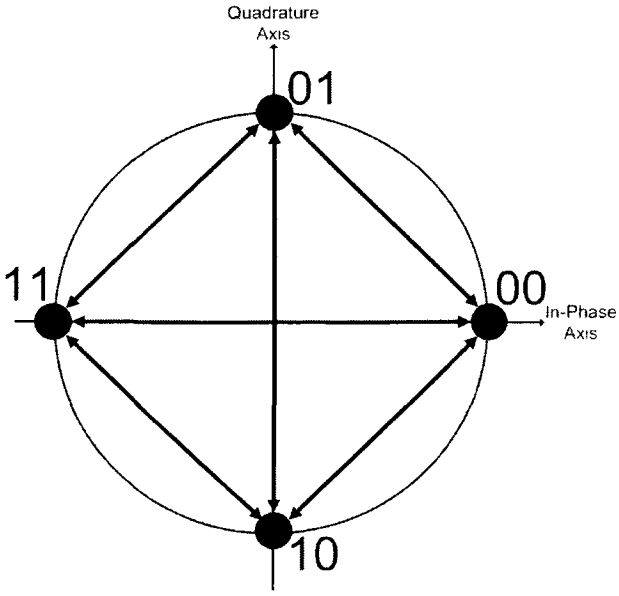

Figure 3.2: Signal space constellation with symbol mapping

where $z(t)$ is the AWGN present in the receiver. As discussed previously, the channels utilized by both signals will have different effects on the phases seen at R, which will also be different from the intrinsic phase at the sources. We assume that R has knowledge of both received carrier phases, θ_1 and θ_2, through the use of a pilot sequence during which each source is able to disjointedly transmit training symbols. Without loss of generality, we assume that R is able to generate a local version of the carrier with phase θ_1. The carrier phase offset between the two signals is given by $\theta_\triangle = \theta_1 - \theta_2$.

The PNC signal demodulator must first convert the received signal sample given by (3.2) to a baseband value. Due to the carrier phase offset, the PNC signal will span the 2-dimensional signal space, even for the case of $M = 2$. The receiver must therefore mix $r(t, a_1, a_2)$ with the orthogonal set of basis functions:

$$c_i(t) = \cos(2\pi f_c t + \theta_1)$$
$$c_q(t) = -\sin(2\pi f_c t + \theta_1)$$

This contrasts with the technique proposed in [3] to demodulate BPSK PNC signals. In their analysis, the receivers use exclusively the in-phase version of the carrier, $c_i(t)$, which

is given phase $\frac{\theta_\triangle}{2}$. However, as the two BPSK signals making up the PNC are phase offset, the full set of basis functions is needed to correctly demodulate the signal.

The receiver proceeds to mix $r()$ with the locally-generated carriers, $c_i(t)$ and $c_q(t)$. After low-pass filtering, it gets the following values

$$\begin{aligned} r_i(a_1, a_2) &= c_i(t) r(t, a_1, a_2) \\ &= \cos(2\pi f_c t + \theta_1)[s_1(t, a_1) + s_2(t, a_2) + n(t)] \\ &= \frac{1}{2}(Re\{y(a_1)\} + \cos(\theta_\triangle) Re\{Y(a_2)\}) - \frac{1}{2}\sin(\theta_\triangle) Im\{y(a_2)\} + z_n \end{aligned} \tag{3.3}$$

and

$$\begin{aligned} r_q(a_1, a_2) &= c_q(t) r(t, a_1, a_2) \\ &= -\sin(2\pi f_c t + \theta_1)[s_1(t, a_1) + s_2(t, a_2) + n(t)] \\ &= \frac{1}{2}(Im\{y(a_1)\} + \cos(\theta_\triangle) Im\{Y(a_2)\}) + \frac{1}{2}\sin(\theta_\triangle) Re\{y(a_2)\} + z_n \end{aligned} \tag{3.4}$$

These 2 orthogonal components constitute the baseband signal value with which the receiver decodes the transmitted symbols,

$$r(a_1, a_2) = r_i(a_1, a_2) + j r_q(a_1, a_2) \tag{3.5}$$

We seek to leverage the benefits of network coding and obtain a joint data from $r()$, not the seperate a_1 and a_2 values. Thus, a mapping $a_{nc} = g(a_1, a_2)$ is needed such that

$$\begin{aligned} & g(a_i, a_j) = g(a_k, a_l) \\ & \text{if} \\ & r(a_i, a_j) = r(a_k, a_l) \quad for \;\; all \;\; i, j, k, l \in 0, 1, ...M - 1 \end{aligned}$$

Furthermore, the mapping must be invertible to allow the receivers to recover their intended information. In the case of $\theta_\triangle = 0$, the following mapping will meet these requirements

$$\begin{aligned} g(a_1, a_2) &= a_1 + a_2 \\ a_{nc} &= a_1 + a_2 \end{aligned} \tag{3.6}$$

with addition carried out over $GF(M)$ (bitwise exclusive-or). Thus,

$$r(a_{nc}) = r(a_1, a_2) = r_i(a_1, a_2) + jr_q(a_1, a_2)$$

By knowing the value of $\theta_\triangle$, the receiver is able to assign a network coded symbol to the possible signal points it can receive and obtain the maximum likelihood estimate of the the transmitted PNC data.

3.3 Symbol Ambiguity

Crosstalk between the quadrature components is present in the complex signal values recovered by the receiver, as seen in (3.3) and (3.4). The in-phase and quadrature components of the PNC baseband signal should only depend on the source data modulating the same axis. This is not the case, as we can see that when $\theta_\triangle \neq 0$, the in-phase term $r_i()$ will depend on the quadrature component of $s_2()$ and vice versa. This crosstalk is the result of the relative rotation of s_2 with respect to s_1 brought on by the different carrier phases. As an illustration of this effect, Figure 3.3 depicts the constellation of a PNC symbols made up of 2 QPSK signals. We can see the effect of carrier phase offset on the orientation of one of the component signals, which is rotated by $\theta_\triangle$ relative to the other component signal. The symbol points are shown along with the PNC data they represent. For example, the symbol point labelled as "A" corresponds to PNC data 10. This value is derived from symbol points of the component signals, $s_1()$ and $s_2()$, which, referring to Figure 3.2, represent data 00 and 10, respectively.

We will now explore the effects of this constellation misalignment by examining the case of symbol ambiguity, which occurs when points in the received signal space correspond to more than one network coded data. We shall consider the case of ambiguity for two different PNC constellation points,

$$r(a_{nc}^1) = r_i(a_1^1, a_2^1) + jr_q(a_1^1, a_2^1)$$

and

$$r(a_{nc}^2) = r_i(a_1^2, a_2^2) + jr_q(a_1^2, a_2^2)$$

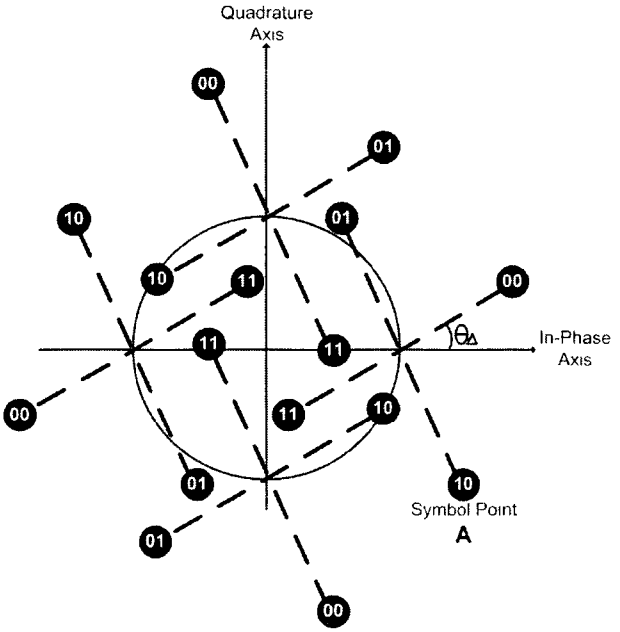

Figure 3.3: PNC constellation for $M = 4$

Definition 3.1. *Signal space points for which*

$$r(a_{nc}^1) = r(a_{nc}^2)$$

and

$$a_{nc}^1 \neq a_{nc}^2$$

experience symbol ambiguity.

We will now elaborate on the conditions under which signal points experience ambiguity.

Theorem 3.1. *The network coded signals experiencing ambiguity must have distinct data components,*

$$\begin{aligned} a_1^1 &\neq a_1^2 \\ a_2^1 &\neq a_2^2 \end{aligned} \tag{3.7}$$

Proof. Consider the case of symbol ambiguity where one of the data components is the

same. for example $a_1^1 = a_1^2$. According to Definition (3.1) we have that

$$\begin{aligned} r(a_{nc}^1) &= r(a_{nc}^2) \\ (c_i(t) + jc_q(t))r(t, a_1^1, a_2^1) &= (c_i(t) + jc_q(t))r(t, a_1^2, a_2^2) \\ s_1(t, a_1^1) + s_2(t, a_2^1) &= s_1(t, a_1^2) + s_2(t, a_2^2) \\ s_1(t, a_1^1) + s_2(t, a_2^1) &= s_1(t, a_1^1) + s_2(t, a_2^2) \\ s_2(t, a_2^1) &= s_2(t, a_2^2) \\ a_2^1 &= a_2^2 \end{aligned}$$

where we have neglected the noise terms $z(t)$ present in the PNC symbols. Thus, the two data components of both PNC symbols must be mapped to the same data and we get $a_{nc}^1 = a_{nc}^2$. The symbols are not ambiguous. □

We will now prove the impossibility of ambiguity for the case of component signals with only two constellation point, $M = 2$.

Theorem 3.2. *When the signals used in the physical network coded system have only two constellation points, no symbol ambiguity is possible at any carrier phase offset.*

Proof. For the case the of $M = 2$, if network coded signal points were ambiguous, we know from Theorem (3.1) that their two component data values must be distinct. Therefore, we have that $a_1^1 + a_1^2 = 1$ and $a_2^1 + a_2^2 = 1$. The network coded data must also be different,

$$\begin{aligned} a_{nc}^1 &\neq a_{nc}^2 \\ a_1^1 + a_2^1 &\neq a_1^2 + a_2^2 \\ a_1^1 + a_1^2 &\neq a_2^1 + a_2^2 \end{aligned}$$

From the first condition, we have that both sides of this last equation are 1, therefore completing the proof by contradiction. □

Thus, BPSK or any binary signal yield physical network coded symbols which cannot be ambiguous. An illustration of a PNC constellation is shown in Figure 3.4. Intuitively,

it is clear that the symbol points representing different data cannot occupy the signal space for any value of phase offset $\theta_{\triangle}$.

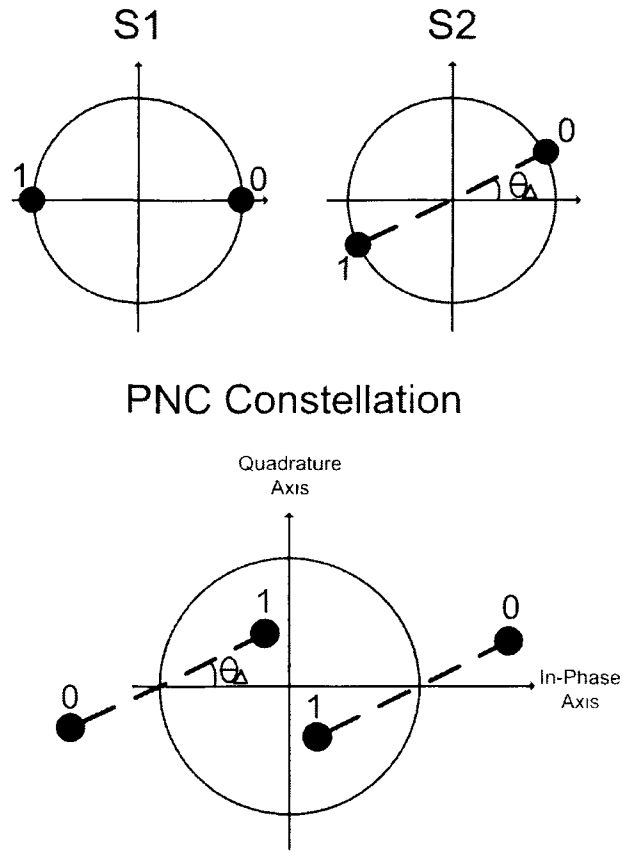

Figure 3.4: Constellation diagrams of the 2 source's BPSK signals and the resulting PNC signal

This result confirms the minimum rate at which PNC symbols can be detected. A PNC symbol must be sampled at the bit rate of the two sources for a reliable decode to follow. In addition, the component signals must only have binary transitions. We will use these observations to obtain a general modulation scheme which avoids the problems arising from carrier phase offset in physical network coding systems.

We will now elaborate on the occurrence of symbol ambiguity for the case of physical network signals made up of M-PSK signals with $M > 2$. From (3.1), we know that the

M-PSK constellations respect the following condition

$$y(a+A) = -y(a) \qquad for \quad a \in 0.1, ...M-1 \tag{3.8}$$

where A is a constant and the addition $a+A$ is carried out over $GF(M)$. Signal points seperated by 180° represent data differing by a constant value, as shown in Figure 3.2.

For the case of $\theta_\triangle = 0°$, symbol ambiguity is avoided since there is no crosstalk between the quadrature components of $r(a_{nc})$. Equivalent symbol points cannot represent different PNC data.

Similarly, for the case of $\theta_\triangle = \pi$, the expressions (3.3) and (3.4) quantifying the received baseband values will lose their crosstalk components. Neglecting the noise terms, we get that

$$\begin{aligned} r_i(a_1, a_2)_{|\theta_\triangle=\pi} &= \frac{1}{2}(Re\{Y(a_1)\} + \cos(\theta_\triangle)Re\{Y(a_2)\}) - \frac{1}{2}\sin(\theta_\triangle)Im\{Y(a_2)\} \\ &= \frac{1}{2}(Re\{Y(a_1)\} - Re\{Y(a_2)\}) \\ &= \frac{1}{2}(Re\{Y(a_1)\} + Re\{Y(a_2+A)\}) \\ &= r_i(a_1, a_2+A)_{|\theta_\triangle=0} \end{aligned}$$

and similarly

$$r_q(a_1, a_2)_{|\theta_\triangle=\pi} = r_q(a_1, a_2+A)_{|\theta_\triangle=0}$$

Thus, at a phase offset of π, the PNC symbols become biased by constant value A relative to their values at 0 phase. As there is no symbol ambiguity at 0 phase offset, there is likewise no ambiguity at π.

However, for $\theta_\triangle = \frac{2\pi\imath}{M}$ for $\imath \in 1, ...M/2-1, M/2+1, ...M-1$, we can prove that the problem of symbol ambiguity arises. To show that ambiguity occurs, let $a_1 = a_2 = 0$. For

example, at offset $\theta_{\triangle} = \frac{2\pi}{M}$, the received baseband values are

$$\begin{aligned}
r_i(0,0) &= \frac{1}{2}(Re\{Y(0)\} + \cos(\frac{2\pi}{M})Re\{Y(0)\} - \sin(\frac{2\pi}{M})Im\{Y(0)\}) \\
&= \frac{1}{2}(1 + \cos(\frac{2\pi}{M})) \\
&= \frac{1}{2}(\cos(\frac{2\pi}{M}) + \cos^2(\frac{2\pi}{M}) + \sin^2(\frac{2\pi}{M})) \\
&= \frac{1}{2}(\cos(\frac{2\pi}{M}) + \cos(\frac{2\pi}{M})\cos(\frac{2\pi(M-1)}{M}) - \sin(\frac{2\pi}{M})\sin(\frac{2\pi(M-1)}{M})) \\
&= \frac{1}{2}(Re\{Y(1)\} + \cos(\frac{2\pi}{M})Re\{Y(M-1)\} - \sin(\frac{2\pi}{M})Im\{Y(M-1)\}) \\
&= r_i(1, M-1)
\end{aligned}$$

and

$$\begin{aligned}
r_q(0,0) &= \frac{1}{2}(Im\{Y(0)\} + \cos(\frac{2\pi}{M})Im\{Y(0)\} + \sin(\frac{2\pi}{M})Re\{Y(0)\}) \\
&= \frac{1}{2}(\sin(\frac{2\pi}{M})) \\
&= \frac{1}{2}(\sin(\frac{2\pi}{M}) - \cos(\frac{2\pi}{M})\sin(\frac{2\pi}{M}) + \sin(\frac{2\pi}{M})\cos(\frac{2\pi}{M})) \\
&= \frac{1}{2}(\sin(\frac{2\pi}{M}) + \cos(\frac{2\pi}{M})\sin(\frac{2\pi(M-1)}{M}) + \sin(\frac{2\pi}{M})\cos(\frac{2\pi(M-1)}{M})) \\
&= \frac{1}{2}(Im\{Y(1)\} + \cos(\frac{2\pi}{M})Im\{Y(M-1)\} + \sin(\frac{2\pi}{M})Re\{Y(M-1)\}) \\
&= r_q(1, M-1)
\end{aligned}$$

Thus, at carrier phase offset $\theta_{\triangle} = \frac{2\pi}{M}$, we have that r(0,0) = r(1,M-1). This implies ambiguity, since

$$a_{nc}^1 = 0 + 0$$
$$a_{nc}^2 = 1 + M - 1$$

Thus,

$$a_{nc}^1 \neq a_{nc}^2$$

The symbol points correspond to different PNC values which the receiver has no way of distinguishing.

3.4 Minimum Distance

We will now quantify the effect of phase offset, $\theta_{\triangle}$, on the distance between symbol points representing different data in the network coded constellation. For the case of $M = 2$, we proved in the last section that symbol ambiguity is impossible. As a corollary to this proof, the minimum distance of these physically network coded symbols will stay constant regardless of the relative orientation of their component constellations. We therefore consider minimum distance for the case of modulations with $M > 2$. We know from the previous analysis that symbol ambiguity occurs at $\theta_{\triangle} = \frac{2\pi i}{M}$. for $i = 1, 2...$, but is avoided at $\theta_{\triangle} = 0, \pi$. Consequently, we can expect that the minimum distance of PNC signals will vary as a function of of $\theta_{\triangle}$.

Figure 3.5 shows the minimum distance as a function of $\theta_{\triangle}$ for physical network codes made up of QPSK and 8-PSK signals. The distance between signal points representing different physically network coded data is normalized by the minimum distance of the component signals. As previously discussed, there is no ambiguity at $\theta_{\triangle} = 0, \pi$. In fact, at these offsets, PNC QPSK has the same minimum distance as the underlying constellation. The analysis of [3], which showed that the capacity of the multiple-access PNC link is similar to the single signal case, holds in this situation. However, a slight shift in the relative carrier phase brings about a steep decline in minimum distance and channel capacity, culminating in total ambiguity at $\theta_{\triangle} = \frac{\pi}{2}$. The results are even more discouraging for the case of 8-PSK, which has $\frac{8^2}{4^2} = 4$ times more points sharing the same signal space. There is an intrinsic performance penalty when using PNC with this modulation, as the minimum distance peaks at a fractional value of the underlying constellation's. Also, ambiguity can be seen at 3 carrier phase offsets in the interval $\theta_{\triangle} \in [0\ \pi]$.

Clearly, the PNC system becomes unworkable when allowing for an arbitrary carrier phase offset between its component signals. The problem of reduced minimum distance and symbol ambiguity result when applying higher-order PSK constellations to PNC. Although we have only considered M-PSK for $M = 4, 8$, these problems will arise when

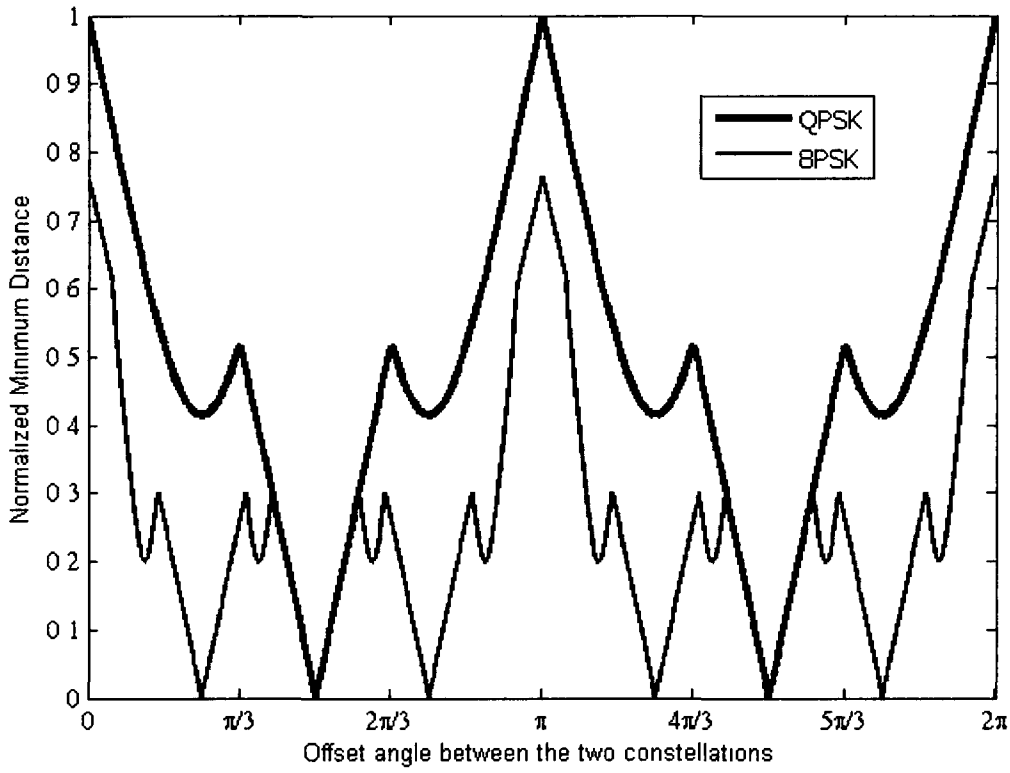

Figure 3.5: Normalized minimum distance of PNC constellations.

using any higher-order phase modulation. We therefore need a modulation scheme and demodulating algorithm which can overcome the problem of phase offset and produce a joint-decode of PNC signals.

Chapter 4

MLSD of bit-Offset PNC

In this section, we present the MLSD algorithm used for the joint detection of signals received simultaneously. As seen in the last section, two signals that are received at the same time must be assumed to have an arbitrary carrier phase offset. For the case of signals with symbol constellations containing more than 2 points, this offset leads to a reduced minimum distance and, in the worst case, total symbol ambiguity. Conversely, physical network codes made up of signals with only 2 constellation points will always have the same minimum distance regardless of carrier phase offset, with the resulting network coded constellation containing at most 4 points. This observation is used to develop higher-order modulation schemes compatible with physical network coding. Since a receiver is able to detect at most 4 constellation points from the two sources at one time, the modulation used by the sources cannot, at a given time instant, branch to more than two values. With the aim of developing higher order modulations and increasing the transmission rate, we allow an arbitrary number of possible symbol points to which a source can eventually transition during a symbol interval. This progressive transition will allow the receiver to track the detected physical network coded signal as it branches at each bit interval.

Bit offset modulations possess these progressive transition properties, of which Offset Quadrature Shift Keying (OQPSK) is a well known variant. In this scheme, the two bits

describing a symbol each modulate separate orthogonal channels. Moreover, the channels are made to transition in value at different times such that at every bit period, the signal constellation either switches value or stays put. However, at each symbol period, the signal can take on all four constellation values. Originally developed for use in a single-user setting, OQPSK's good spectral containment and ease with which it can be amplified led to its widespread adoption. In the case of a multi-user setting, however, we propose to leverage its progressive constellation transitions to enable a receiver to track the phases of 2 OQPSK signals received simultaneously.

This use of offset modulation to enable physical network coding is related to the use of MSK by the ANC scheme [4]. MSK also offsets the modulation of its two quadrature channels such that instantaneous 180° phase transitions are avoided. In addition, MSK benefits from pulse shaping and a continuous phase impulse response which further ease its amplification. Practically, MSK can be viewed as employing $\pm\frac{\pi}{2}$ phase transitions to transmit different bits. It therefore also achieves a capacity of 2 bits/s/Hz while having only binary transitions at every time instant, precluding the occurrence of symbol ambiguity when used for physical network coding with the proposed MLSD algorithm. This avoidance of symbol ambiguity was not the motivation of the authors, however, who intended ANC as a practical proposal which foregoes all synchronization assumptions [4]. This was shown possible with a completely non-coherent detection strategy which circumvents the problem of ambiguity inherent in the coherent detection of PNC signals. Nevertheless, the MLSD of physical network coded signals could be adapted to work with MSK.

4.1 Offset Quadrature Phase Shift Keying

Returning our attention to OQPSK, we can model a signal sample using the following:

$$s(t) = \sqrt{\frac{\xi_b}{T_b}} a_I \cos(2\pi f_c t) + \sqrt{\frac{\xi_b}{T_b}} a_Q \sin(2\pi f_c (t - T_b)) \qquad for \quad 0 \leq t < T, \tag{4.1}$$

where ξ_b is the energy per bit, T_b the bit duration and f_c the carrier frequency. The transmitted data is reflected in the a_I and a_Q terms, which modulate the in-phase and quadrature channels, respectively. The timing difference between the quadradure channels is evident in the time shift of one with respect to the other. This modulation can be seen in Figure 4.1. The modulating symbol's leftmost and rightmost bit modulate the in-phase and quadrature channels, respectively.

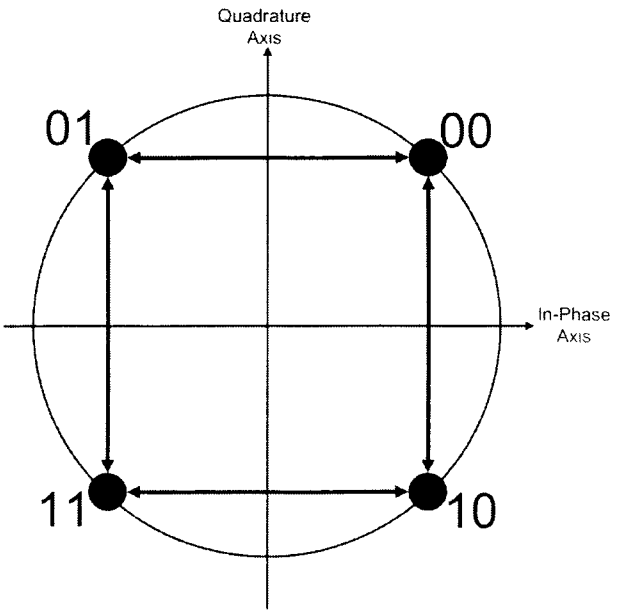

Figure 4.1: OQPSK constellation

Equation (4.1) can be further refined to reveal the phase states of OQPSK. Following the derivations of Simon *et al.* [23], we now express a signal sample using:

$$s(t) = \sqrt{\frac{\xi_b}{T_b}} \exp(2\pi f_c t + \phi(t, \alpha) + \theta) \qquad for \quad 0 \leq t < T_s \tag{4.2}$$

where θ is an arbitrary carrier offset phase. The phase modulation is reflected in the $\phi()$ term, which is given by:

$$\phi(t, \alpha) = 2\pi h \sum_n \alpha_n q(t - nT_b) \tag{4.3}$$

where n is the discrete time index corresponding to the bit intervals, h is the modulation index, assumed $\frac{1}{2}$ for OQPSK, and $q(t)$ is the pulse shape. The sequence $\alpha_n \in \{-1, 0, +1\}$

is related to the input bitstream $a_n \in \{-1, +1\}$ by:

$$\alpha_n = \frac{1}{2}(-1)^n a_{n-1}(a_n - a_{n-2}) \tag{4.4}$$

Further simplification in relating the phase state to the received symbol value is possible for the case of OQPSK, which has an instantaneous phase response. Indeed, $q(t)$ can be modelled as a step function of amplitude $\frac{1}{2}$, resulting in $\phi()$ changing value at discrete bit intervals only. We can therefore rewrite (4.3) as:

$$\phi(\alpha_n) = \frac{\pi}{2}\alpha_n + \phi(\alpha_{n-1}) \tag{4.5}$$

From this last equation, the recursive state representation of OQPSK becomes readily apparent. As shown by [23], the states are described by the previous 2 bits, a_{n-1} and a_{n-2}, as well as by n, which can be even for in-phase transitions or odd for quadrature transitions. The trellis representation of OQPSK's state transitions is shown in Figure 4.2. The signal phase states are shown with values $s \in \{0, \frac{\pi}{2}, \frac{3\pi}{2}, \pi\}$ and represent the transmitted phase relative to the initial signal phase. Also shown are the a_i input bit values which lead to the corresponding state transitions. A time-varying trellis is used to model the progression, as different transitions are taken in the even and odd bit intervals.

4.2 Physical Network Coded OQPSK

We consider the physical network code applied to the system shown in Figure 3.1. The summation signal $r(t)$ received by T is given by:

$$r(t) = s_1(t) + s_2(t) + z(t) \tag{4.6}$$

where $s_i(t)$, $i \in 1, 2$ are the OQPSK signals transmitted by sources $X1$ and $X2$. The AWGN of the receiver is captured by the $z(t)$ term, which is a Gaussian random process of power spectral density N_0. In addition to AWGN, wireless links are usually modeled as having a channel effect. While the effects on the received amplitude have been ignored, the effect on received phase is accounted for implicitly by the arbitrary carrier phase we

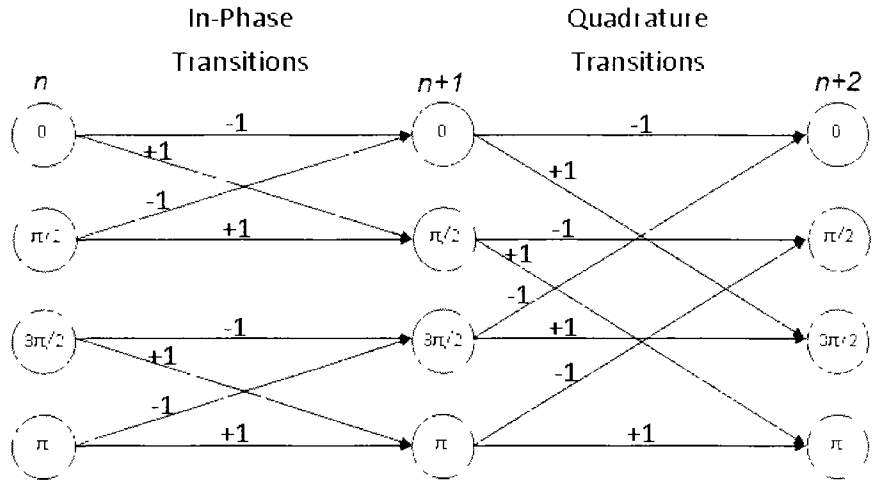

Figure 4.2: OQPSK trellis representation

give to both signal components of (4.6). Applying the definition equation of OQPSK (4.1) and assuming equal transmit power by both sources, we get the following expression:

$$r(t) = \sqrt{\frac{\xi_b}{T_b}} \exp\left(\jmath(2\pi f_c t + \phi(\alpha_n^1) + \theta_1)\right) + \sqrt{\frac{\xi_b}{T_b}} \exp\left(\jmath(2\pi f_c t + \phi(\alpha_n^2) + \theta_2)\right) + z(t) \quad (4.7)$$

where θ_1 and θ_2 are the received phases of the signal components coming from $X1$ and $X2$, respectively. Similarly, the α_n^1 and α_n^2 terms represent the modulating data of both sources at the n^{th} time interval.

The receiver is assumed to have knowledge of both sources' received carrier phases through the use of a training sequence during which each source is able to transmit a pilot symbol. Thus, destination T is able to mix a locally-generated carrier which is assumed, without loss of generality, to have phase θ_1, with $r(t)$ to obtain the following baseband signal:

$$r_n = \sqrt{\frac{\xi_b}{T_b}} \exp\left(\jmath(\phi(\alpha_n^1))\right) + \sqrt{\frac{\xi_b}{T_b}} \exp\left(\jmath(\phi(\alpha_n^2) + \theta_\Delta)\right) + z_n \quad (4.8)$$

where $\theta_\Delta = \theta_2 - \theta_1$ is the difference between the two sources' carrier phases.

4.3 Trellis Representation of PNC signals

In order to perform MLSD on the received signal set R, it is necessary to define the trellis that models the progression of the received physically network coded symbols. As the underlying signals have a constrained state progression, the aggregate symbols will likewise possess a patterned succession.

Similar to the case of single-source OQPSK, the PNC signal states are defined by the phase values at every time interval. Specifically, we define the states of the PNC signal in terms of the phase states of the two transmitted component symbols:

$$S_k, E_k \in \sqrt{\frac{\xi_b}{T_b}}[(\exp(\jmath\phi(a_n^1)) + \exp(\jmath(\phi(a_n^2) + \theta_\Delta))] \quad for \quad k = 1, 2, ...16$$

where S_k and E_k are the starting and ending states at the n^{th} bit interval, respectively. The state values are a function of the $\phi(a)$ modulating terms which were shown in (4.4) to depend on the last 2 transmitted bits. We therefore express the k index as a function of the last two bits transmitted by the two sources.

$$k = \begin{cases} f(a_{n-1}^1, a_n^1, a_{n-1}^2, a_n^2) & \text{if } n \text{ is even} \\ f(a_n^1, a_{n-1}^1, a_n^2, a_{n-1}^2) & \text{if } n \text{ is odd} \end{cases} \tag{4.9}$$

where $f()$ is a counting function that returns the state number given 4 binary values. The state progression corresponds to a time-varying trellis that is similar to the underlying alternating transitions of OQPSK and explains the different ordering of the a parameters in (4.9). So, for example, if the last 2 bits transmitted by $X1$ and $X2$ are $a_n^1, a_n^2 = -1$ and the interval is even, the starting state will be S_1 and the possible ending states are $\{E_1, E_2, E_5, E_6\}$. Likewise, if the interval is odd, the starting state will be S_1 and the possible ending states are instead $\{E_1, E_3, E_9, E_{11}\}$. An illustration of this trellis is shown in Figures 4.3 and 4.4. The relative phase states of the two component signals are also displayed.

A good way to visualize the PNC trellis is to decompose it into sets. At each interval, the 16 states are divided into 4 sets, each containing 4 states. The signal points corresponding to set A of the in-phase transition is shown in Figure 4.5. The effect of phase

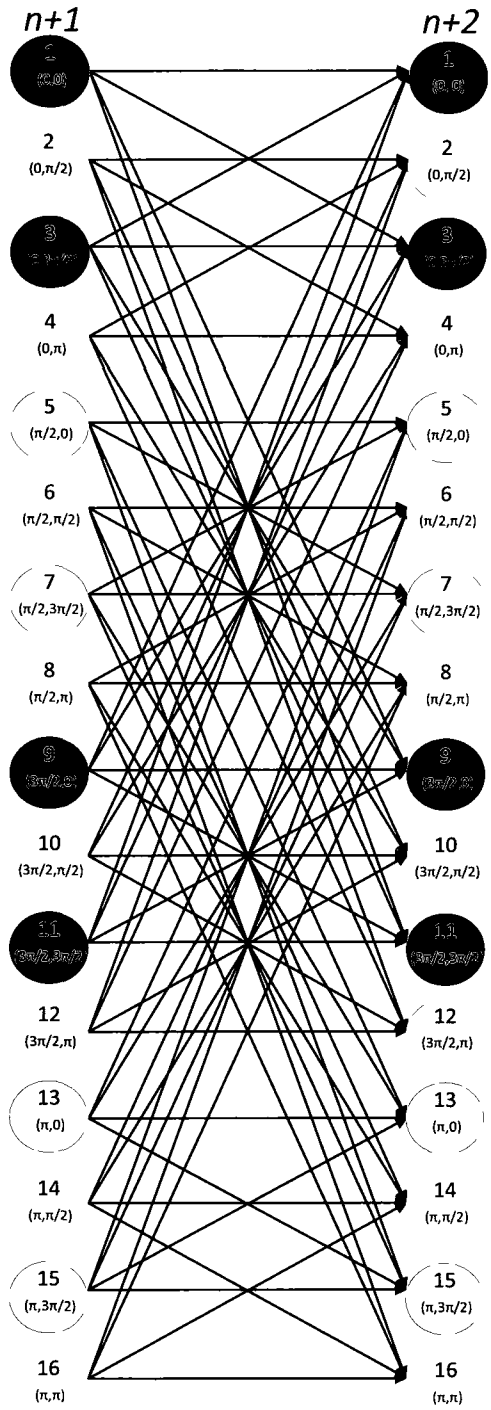

Figure 4.4: Trellis state progressions for PNC OQPSK: quadrature transitions

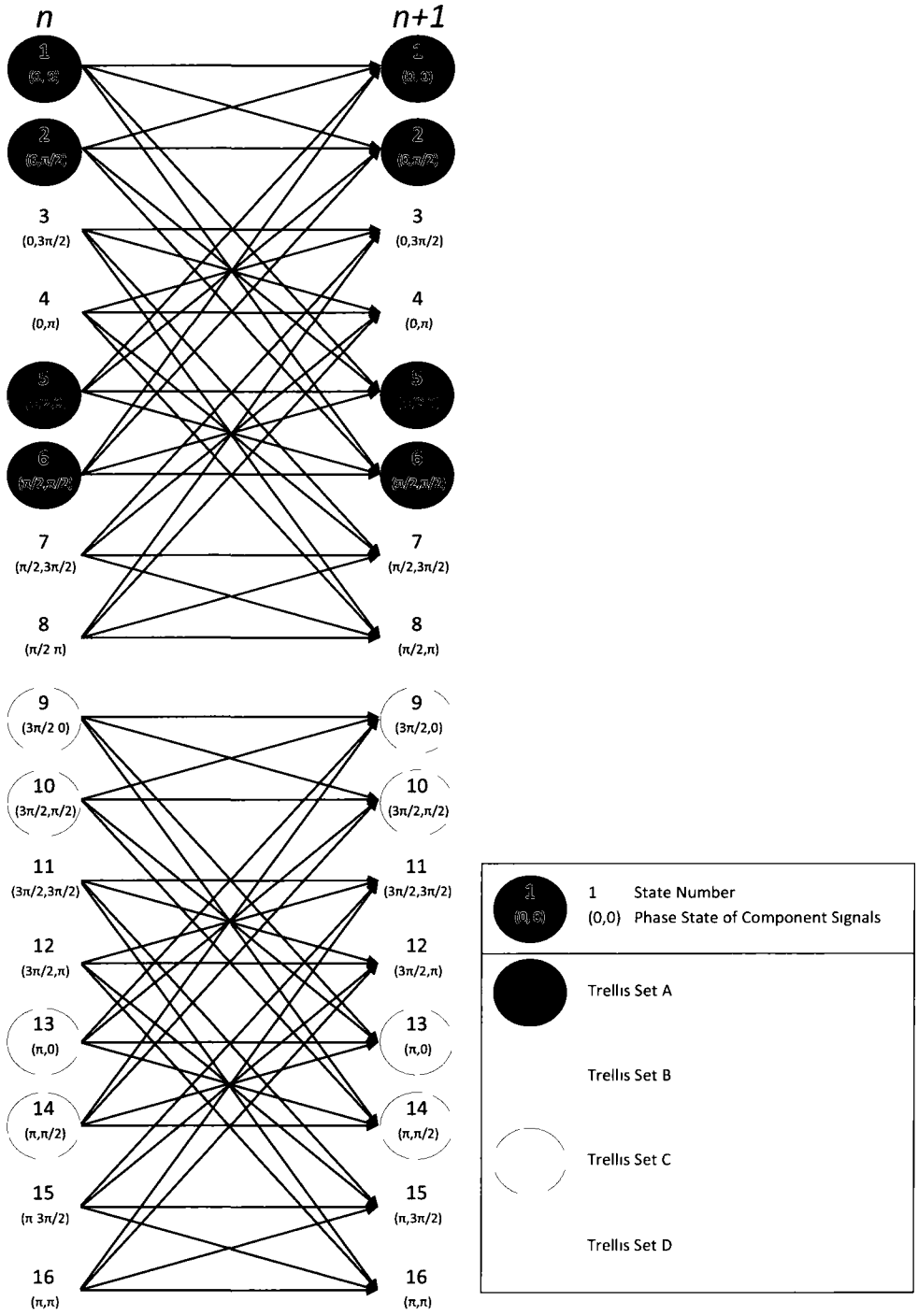

Figure 4.3: Trellis state progressions for PNC OQPSK: in-phase transitions

offset $\theta_\triangle$ on the layout of the signal points, which are marked with their corresponding PNC data, is clearly depicted. For every starting state in a set, $S_k \in \Lambda$, the ending state for each transition is also in the same set, $E_j \in \Lambda$. There is a crossover in states, however, as the in-phase and quadrature transitions have different sets. Indeed, in the next time interval, $\exists j$ such that $S_j = E_j$ and $S_j \notin \Lambda$. The significance of sets will become apparent in the next section when they will be used to obtain a heuristic explanation for the BER of the MLSD.

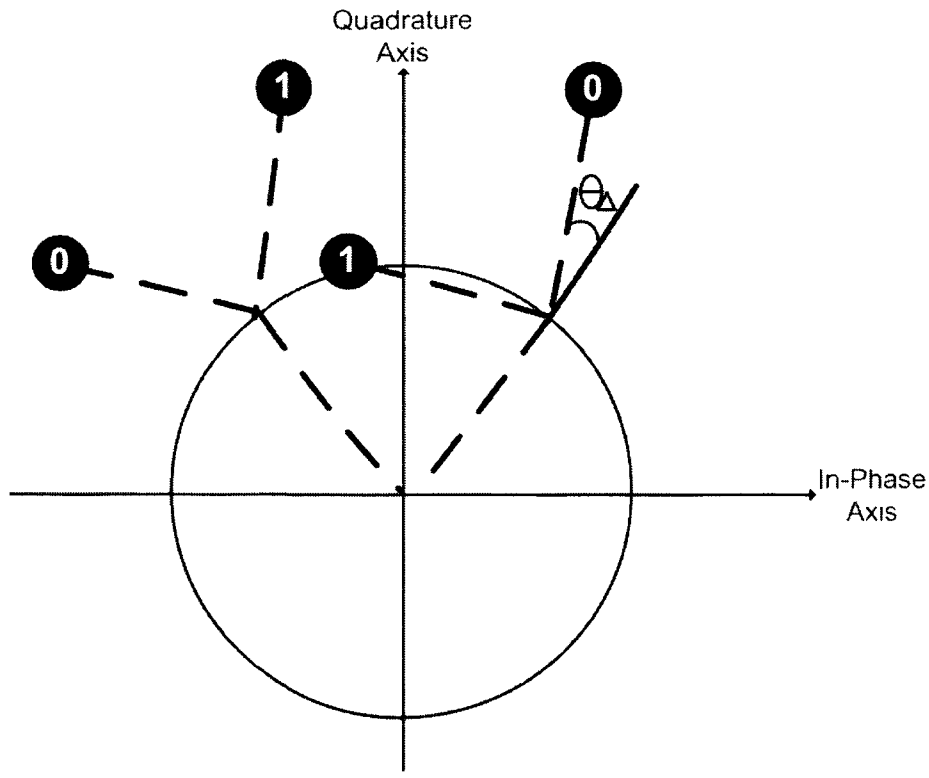

Figure 4.5: PNC constellation corresponding to Set 1 of the in-phase transition

The decoder is able to use this trellis model to perform the MLSD of the transmitted network coded data. Given the set of received symbols R, the decoder seeks to obtain the sequence of states S which maximizes the *a posteriori* probability given by:

$$p(R|S) = \frac{1}{\sqrt{2\pi}\sigma} \exp\left(-\frac{[R-S]^2}{2\sigma^2}\right) \tag{4.10}$$

where $\sigma^2 = \frac{1}{2}N_0$ is the variance of the AWGN. The Viterbi Algorithm (VA) is a practical

method of obtaining this maximum likelihood sequence. As the trellis is based on OQPSK, the branch metrics can be similarly computed by comparing the ending states to the received samples at every bit interval, independent of the originating state and transition taken for each branch. Rearranging (4.10) by discarding the terms common to every state and by computing the log-likelihood, we get the following the branch metric equation:

$$\mu_n^k = (r_n - E_k)^2 \tag{4.11}$$

where μ_n^k is the branch metric for transitions ending at state k and occuring at bit interval n. The decoder uses these metrics to progress its confidence in every state at each bit iteration:

$$\lambda(E_k) = \lambda(S_j) + \mu_n^k \tag{4.12}$$

where $\lambda()$ represents the cumulative metric of the given state. The index j refers to the states for which $S_j \in \Lambda$ if $E_k \in \Lambda$; *i.e.*, the starting and ending states are in the same set. The VA is used to compute the confidence of each state and select the survivor path with the smallest cumulative metric, from which the network coded data readily follows. The network coding constraint requires that the mixed symbol be extracted from the received signal and therefore that the receiver decode a value corresponding to the multiplication of both sources' symbols. Therefore, all states with indexes for which $a_n^1 \neq a_n^2$ yield the decoded network coded data $\hat{a_n^{nc}} = -1$. Conversely, states for which $a_n^1 = a_n^2$ yield $\hat{a_n^{nc}} = 1$

4.4 Generalization of the MLSD

The MLSD of physically network coded OQPSK signals has been presented to resolve the problem of symbol ambiguity for transmission rates of 2 bits/symbol. We now take the concept one step further and adapt it to signals operating with higher order modulations.

In order to carry out MLSD on PNC symbols, the 2 sources are constrained to use bit-offset modulation. We consider M-ary phase and amplitude modulations that are able to spread out their symbol transitions over M bit intervals such that the resulting

bandwidth is not greater than the original modulation's bandwidth. For example, for the case of M=4 just examined, it is a well known fact that OQPSK has a bandwidth equal to that of QPSK. For the case of $M > 4$, additional channels are needed to supplement the in-phase and quadrature channels used by OQPSK. A natural progression is to use an amplitude channel, giving an Offset Quadrature Amplitude Modulation (OQAM).

The receiver must track an increased number of states. Indeed, given an M-ary phase and amplitude modulation, the resulting PNC symbols contain M^2 states representing every combination of the component signals, given by:

$$S_k, E_k \in \sqrt{\frac{\xi_n^1}{T_b}} \exp(\jmath\phi(\alpha_n^1)) + \sqrt{\frac{\xi_n^2}{T_b}} \exp(\jmath(\phi(\alpha_n^2) + \theta_\Delta) \quad for \;\; k = 1, 2, ...M^2$$

where α_n^i and ξ_n^i are the phase and amplitude states, respectively, of the source $i \in 1, 2$ signal during bit interval n. The receiver must also keep track of varying state transitions at every bit interval. As seen for the case of OQPSK, the PNC symbols are modelled with a time-varying trellis that accounts for the alternating in-phase and quadrature transitions. For $M > 4$, there are additional sets of state transitions that signal the remaining bit transmissions. As an example of this generalization, we present PNC for the case of M=8, Offset 8QAM. An illustration of the signal space of this modulation is shown in Figure 4.

The 8QAM constellation is closely linked to the OQPSK signal of the previous section. The 8 symbol points are divided into 2 rings of different diameter, each containing 4 points. The two rings have a $\frac{\pi}{4}$ relative offset and are given symbol values that differ by the leftmost bit.

Analogous to OQPSK, bit offset 8QAM works by also using the in-phase and quadrature transitions to transmit the 2 rightmost symbol bits. However, the third symbol bit is signalled by combining a transition to the other ring amplitude with a $\pm\frac{\pi}{4}$ phase shift. This yields the following modulation:

$$s(t) = [\Omega e^{\jmath\frac{\pi}{4}}]^{\beta(a_{n+3})}\Gamma(t) \tag{4.13}$$

where Ω is the signal amplitude and $\Gamma(t)$ is the component OQPSK modulation given by

$$\Gamma(t) = \exp(2\pi f_c t + \phi(t, \alpha_n) + \theta) \qquad for \;\; 0 \leq t < T_s$$

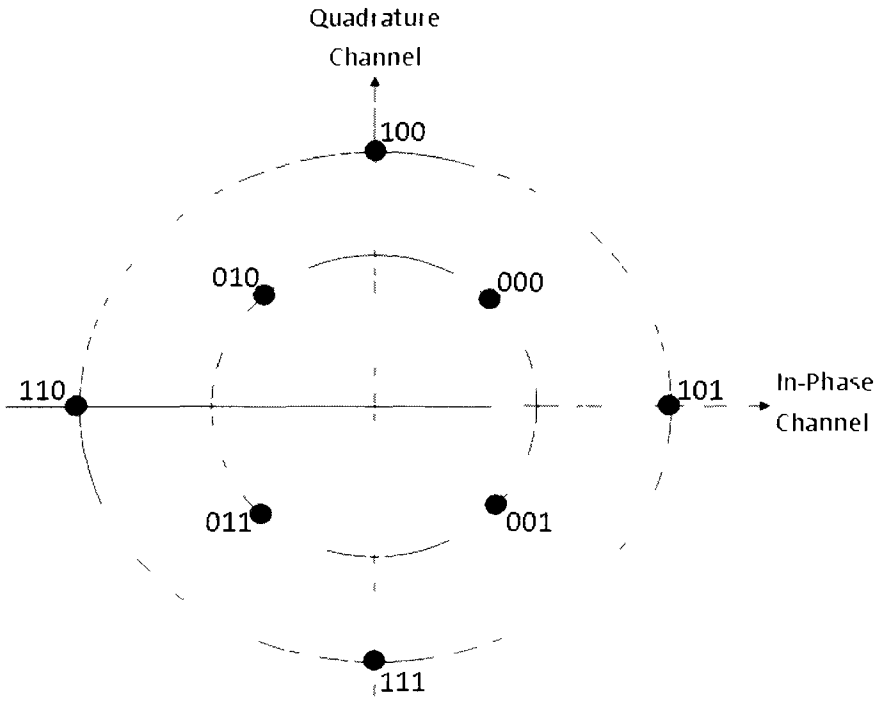

Figure 4.6 8QAM constellation

where

$$a_n = \frac{1}{2} a_{n-2}(a_n - a_{n-3}) \quad for \quad n = 1, 4, 7,$$

and

$$a_n = -\frac{1}{2} a_{n-1}(a_n - a_{n-3}) \quad for \quad n = 2, 5, 8$$

The $\phi()$ term represents the phase modulation and is given by Equation (4.5). The $\beta(a_{n+3})$ term represents the additional amplitude modulation and is given by

$$\beta(a_n) = \frac{1}{2}(a_n + a_{n-3}) + \beta(a_{n-3}) \quad for \quad n = 3, 6, 9.$$

Finally, the Ω term of (4.13) represents the amplitude of the bit samples and follows

$$\sqrt{\frac{\xi_b}{T_b}} = \frac{1}{2}(\Omega + \Omega^{-1})$$

Typically, the outer ring is at twice the amplitude, leading to

$$\Omega = 2\Omega^{-1}$$

As described previously, the receiver obtains the sum of two signals, $s_1(t)$ and $s_2(t)$, with each having an arbitrary carrier phase. The samples are then converted to baseband and given to a $8^2 = 64$ state time-variant trellis decoder, from which a maximum-likelihood estimate of the physical network coded data is obtained.

Refinement of this system will be required, as the offset 8-QAM used by the 2 sources does not respect the bandwidth constraints of the PNC system. The two quadrature channels change in value more than once during a symbol interval, causing the signal bandwidth to exceed that of regular 8-QAM. However, using the Continuous Phase Modulation framework [23], the symbol transitions of 8QAM could be converted into 3 binary transitions that conserve the bandwidth properties of the original modulation.

Chapter 5

Performance Evaluation

In this section, we present the simulation results of the proposed MLSD algorithm used to decode physical network coded data. The system examined is illustrated on Figure 3.1 and consists of two sources simultaneously transmitting to one receiver, which must extract the joint information from the received interference signal. The two sources are assumed to possess perfect timing and frequency synchronization. Additionally, the transmitters use an identical pulse shape and equal transmit power. However, the parameter most difficult to synchronize is the received carrier phase of both component signals. It is on this asynchrony that we focus our attention. Monte Carlo methods are used to produce the receiver AWGN samples.

In the model investigated, we evaluate the decoding of a signal sample given by:

$$r(t) = s_1(t) + s_2(t) + z(t) \tag{5.1}$$

where $z(t)$ is the AWGN and $s_i(t)$ the component signals, for which we consider several different constellations. The destination R must recover the PNC data from received samples $r(t)$ in the presence of carrier offset, which has the effect of rotating $s_2(t)$ relative to $s_1(t)$.

We begin by showing the effects of carrier phase offset on the regular reception of PNC symbols made up of phase modulated signals. We next present the simulation results of the proposed MLSD of OQPSK PNC, which we justify heuristically. Finally, we discuss

the results of the MLSD of PNC symbols made up of offset 8QAM.

5.1 Regular Detection of BPSK PNC

We consider a regular detection strategy for PNC symbols made up of phase modulated signals. This strategy is carried out by building a signal space constellation to which received signal samples are compared. For the case of PNC symbols made up of BPSK signals, the received constellation is shown in Figure 3.4. The receiver is able to obtain the maximum-likelihood estimate of the transmitted data by choosing the PNC symbol point which comes closest to the received signal sample. Figure 5.1 shows the experimental curves of the BER as a function of offset angle betwen the two BPSK signals making up the PNC The SNR value $\frac{\xi_b}{N_0}$ was given three different values, 1, 3 and 5 dB.

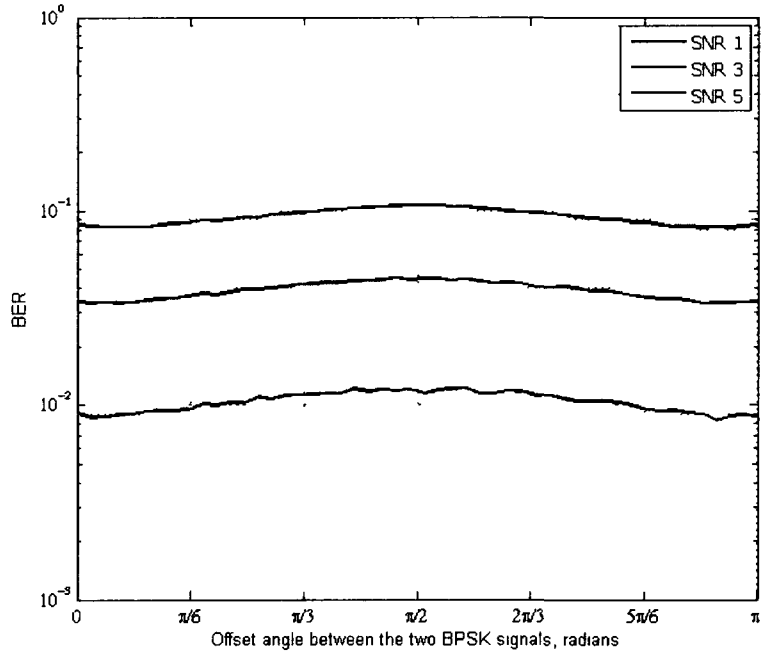

Figure 5 1 PNC detection of BPSK: BER vs offset angle for different values of SNR ($\frac{\xi_b}{N_0}$) in dB

As shown in the previous section, the minimum distance of PNC symbols made up of binary signals is constant at any phase offset. Therefore, we expect a flat BER curve plotted as a function of $\theta_{\triangle}$. Experimental results, however, show a slight deviation in the curves. This can be explained by the increased number of points present in the symbol space as $\theta_{\triangle}$ shifts in value. Indeed, as the carrier offset deviates from 0°, the PNC constellation goes from 3 to 4 points. Correspondingly, the error region increases in size, reaching a maximum at an offset of $\frac{\pi}{2}$. This expansion of the error region results in a linear and negligible increase in the probability of error. A PNC system employing a binary angle modulation is able to avoid the problem of capacity outage when the carrier phases are offset.

5.2 Regular Detection of QPSK PNC

This optimistic result does not hold for higher order phase modulations, however. Previously, it was shown that PNC made up of signals with constellations containing more than 2 symbol points suffer from a reduced minimum distance as one constellation rotates relative to the other.

We now consider PNC applied to QPSK signals. The decoder of such signals works as before. The PNC constellation is compared to the received samples and the closest symbol is chosen as the most likely transmitted network coded data. The PNC QPSK constellation now contains up to 16 points. An example of this constellation is pictured on Figure 3.3.

To illustrate the effects of phase offset on the decoding of PNC QPSK, we again simulate a receiver subject to AWGN. The resulting BER curves are shown in Figure 5.2 for 3 simulated $\frac{\xi_b}{N_0}$ values of 1, 5 and 10 dB.

As predicted by the minimum distance plot of PNC QPSK shown in Figure 3.5, the symbol decode is severely degraded as the carrier offset deviates from 0°. The error region now increases exponentially and peaks at offset multiples of $\frac{\pi}{2}$, where the PNC constellation experiences symbol ambiguity and the decoder is not able to obtain satisfactory

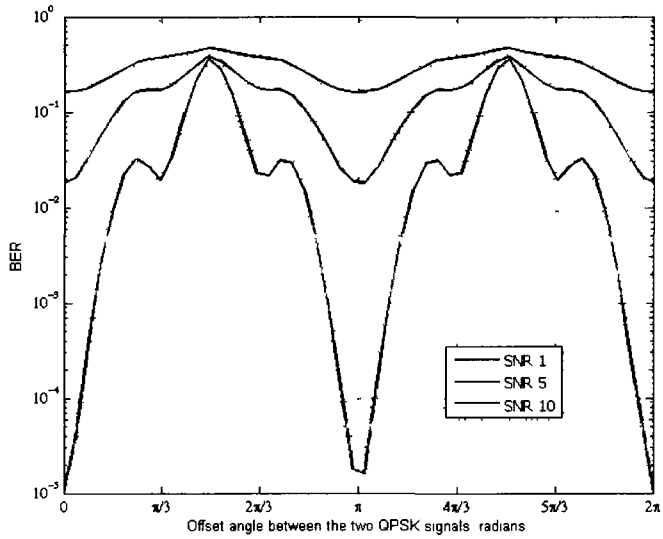

Figure 5.2: PNC detection of QPSK: BER vs offset angle for different values of SNR ($\frac{\xi_b}{N_0}$) in dB

performance at any SNR. Moreover, the BER curves are periodic at an offset of π radians, as with the previous PNC BPSK curves.

Obviously, adapting higher-order modulations to PNC is also impractical. From previous analysis, PNC 8-PSK constellations have an even greater susceptibility to ambiguity and reduced minimum distance. The BER that results from the demodulation of higher-order PNC constellations will exhibit a similar exponential degradation in performance as the phase offset deviates from 0°.

5.3 Proposed Solution Results: OQPSK PNC

Simulation results confirm the previous analysis and demonstrate that employing a modulation rate greater than 1 bit per transmission for PNC yields an unworkable system. The proposed solution consists of bit offset modulation by the sources and MLSD of the resulting PNC symbols by the receiver.

This solution was simulated for a receiver subject to AWGN. Although the wireless

media will invariably result in a fading gain on received signals, we neglect these channel effects and focus instead on the problems brought on by asynchrony Furthermore, we consider unfiltered pulses such that the signal enegy is spread out evenly throughout the symbol duration Even though practical systems would use filtered pulses which have better spectral characteristics, we focus on unfiltered pulses as they are easier to simulate and illustrate the same system properties The resulting decoder performance is illustrated in Figure 5 3, which shows the BER of the PNC decoder for several values of received carrier offset At least 10 bit errors were counted for each experimental point

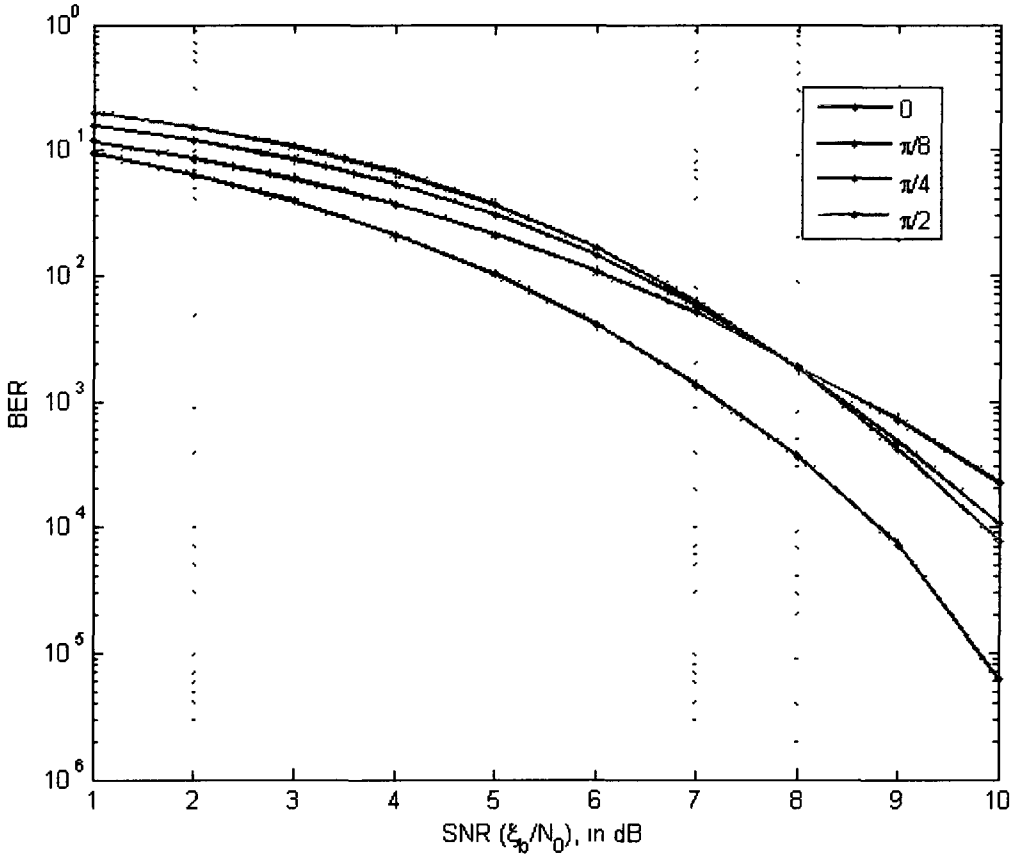

Figure 5 3 Decoder performance of the MLSD of OQPSK for different values of $\theta_\triangle$

The first conclusion from these results is that the MLSD of PNC made up of bit

offset modulated signals is able to solve the problem of symbol ambiguity and decreased minimum distance. There is no carrier phase offset at which the component signals yield PNC symbols which are decoded with a prohibitive performance penalty. In other words, there are no pair of offset values that yield decoder performances that differ by orders of magnitude.

The system does not have an offset-invariant performance, however. There are indeed noticeable differences in the simulated BER curves at different offset values. Figure 5.4 provides another perspective on these results. The decoder BER is now expressed as a function of the offset angle and curves are given for various SNR values. The different curves share certain characteristics: they all have minimum BER results at $\theta_{\triangle} = 0$ and have a structure that is periodic about offset value $\theta_{\triangle} = \frac{\pi}{2}$.

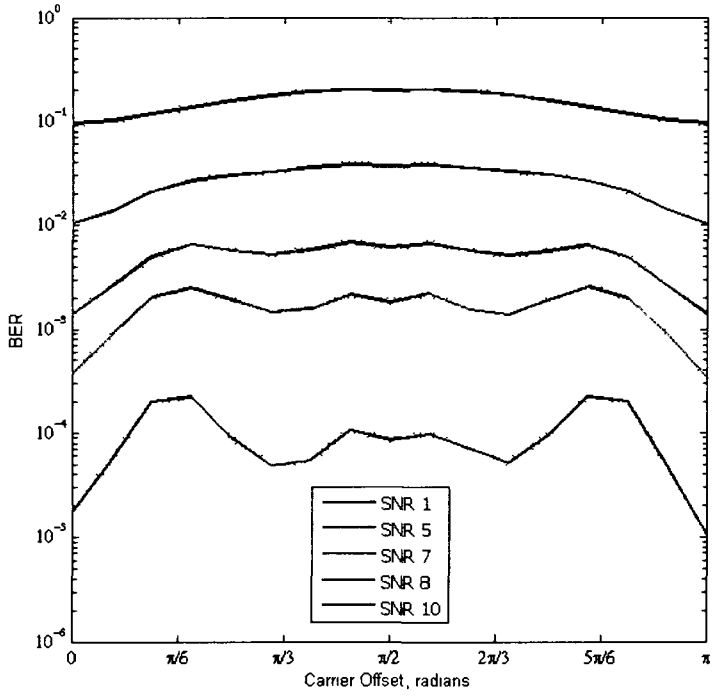

Figure 5.4: MLSD of bit-offset OQPSK: BER as a function of $\theta_{\triangle}$ for different values of SNR ($\frac{\xi_b}{N_0}$) in dB

Interestingly, the curves also have some variable features. For example, at low SNR, the decoder performance at an offset of $\theta_{\triangle} = \frac{\pi}{4}$ is superior to the performance at $\theta_{\triangle} = \frac{\pi}{2}$. However, when the SNR is increased, the results are now opposite as the offset of $\theta_{\triangle} = \frac{\pi}{2}$ yields a better decoder performance.

5.4 Error Bounds on the MLSD of PNC

This behaviour can be explained by analyzing the error events of the trellis decoder. We examine the most-likely error events and obtain heuristic explanations for the varying performance at different values of $\theta_{\triangle}$. The most likely error events are the ones which possess the minimum Euclidean distances to the transmitted sequence. An error event is broken down into 3 phases, described by the path taken on the trellis relative to the real transmitted sequence. The first phase is the initial diverge, during which the two paths start from the same state but end at a different state. The initial phase follows:

$$S_c = S_e$$

$$and$$

$$E_c \neq E_e$$

where S_c and S_e are the starting states of the correct and erroneous sequences, respectively. Similarly, E_c and E_e are the ending states of the corresponding sequences. As the two signals making up the PNC symbols are in effect binary, our previous conclusion that a constant minimum distance holds at every $\theta_{\triangle}$ value applies to this case. The distance between these two paths is $\sqrt{2E_b}$ for every value of $\theta_{\triangle}$. The intermediate phase follows and occurs when the two sequences have starting and ending states which do not belong to the same state sets:

$$\Lambda_c \neq \Lambda_e$$

$$and$$

$$\Sigma_c \neq \Sigma_e$$

where $S_c \in \Lambda_c$ and $S_e \in \Lambda_e$ are the sets of the starting states of the correct and erroneous sequences, respectively. Likewise, $E_c \in \Sigma_c$ and $E_e \in \Sigma_e$ are the sets of the ending states of the corresponding sequences. This intermediate phase can have distance metrics as low as 0 for $\theta_\triangle = \frac{\pi}{2}$.

Finally, the remerge phase completes the error sequence and occurs when the paths of the two branches end at states which belong to the same set, giving

$$\Lambda_c \neq \Lambda_e$$

$$and$$

$$\Sigma_c = \Sigma_e$$

After this remerge phase, the Viterbi decoder will select the error sequence and discard the correct path if the metric of the former is less than the metric of the latter.

Consider the distance metrics associated with the following three $\theta_\triangle$ values shown in Table 5.1, which are derived from the trellis shown in Figures 4.3 and 4.4.

Table 5.1: Distance values of the error phases

$\theta_\triangle$	**Diverge,** d_d^2	**Intermediate,** d_i^2	**Remerge,** d_r^2
0	$2E_b$	$4E_b$	$2E_b$
$\frac{\pi}{4}$	$2E_b$	$(2-\sqrt{2})^2 E_b$	$2(2-\sqrt{2})E_b$
$\frac{\pi}{2}$	$2E_b$	0	$2E_b$

The SNR-variant behaviour of the MLSD becomes immediately clear from the distance values in Table 5.1. It is known that a coded transmission having the largest total minimum distance will perform better at low SNR. However, at high SNR, the largest instance of minimum distance now dominates and the coded sequence possessing this transmission will exhibit the better decode. This explains the experimental results: at low SNR, the decode of PNC symbols with $\theta_\triangle = \frac{\pi}{4}$ is superior to that of $\theta_\triangle = \frac{\pi}{2}$. As the SNR increases and the single instance of minimum distance dominates, the decoding of

the latter outperforms the decoding of the former. Also, the distance values of PNC at $\theta_{\triangle} = 0$ are larger than at the other 2 offsets. This again corroborates the experimental results, as the best decode is obtained at an offset of $\theta_{\triangle} = 0$.

5.5 MLSD of Offset 8QAM PNC

In an effort to generalize the proposed PNC demodulation solution and adapt it to higher-rate transmissions, the MLSD algorithm was applied to PNC waveforms made up of offset 8QAM signals.

We again consider the decoder performance of the receiver of PNC signal samples given by (5.1). The two sources are now transmitting offset 8QAM signals, and $s_1(t)$ and $s_2(t)$ are given by (4.13). The received samples are given to the MLSD described in section 4.4 and the probability of error of the decode is shown in Figure 5.5.

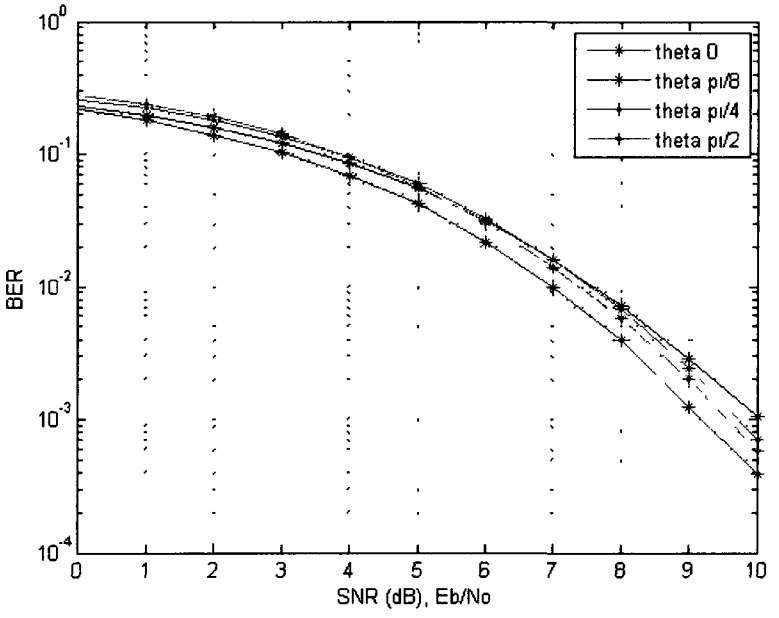

Figure 5.5: Probability of bit error for the MLSD of PNC 8QAM

The results again confirm that the proposed solution is able to solve the problem

of reduced minimum distance and symbol ambiguity for phase-offset physical network coded 8QAM signals. There is no offset at which the decoder experiences an exponential degradation in performance.

As for the case of PNC OQPSK, the performance at the different offsets is also SNR-variant. For example, the order of the quality of the decoding of 8QAM PNC signals at 0dB SNR is given by $[0.\frac{\pi}{8}, \frac{\pi}{4}, \frac{\pi}{2}]$. This order changes to $[0.\frac{\pi}{2}, \frac{\pi}{4}, \frac{\pi}{8}]$ at 10dB SNR. The varying minimum distances through the trellis for the different offset values is again responsible for this behaviour.

The 8QAM error probability curves at the different offsets are much more tightly spaced than for the case of OQPSK. For instance, at 10dB SNR, the BER curves of the MLSD of the PNC 8QAM constellations have a spread of less than 1dB between the best and worst performance. As seen in Figure 5.3, the curves of PNC OQPSK have a spread of almost 2dB at the same SNR.

This smaller variance in performance of offset 8-QAM PNC relative to OQPSK is the result of the larger minimum distances between the different sets making up the trellis. The third transitions, which modulate the amplitude channel of the 8-QAM constellation are less vulnerable to reduced minimum distance as the component constellations rotate relative to each other.

Chapter 6

Conclusion

This section concludes the thesis. We first provide a summary of the contributions and follow with a description of further research in the area of physical network coding.

6.1 Contributions

The contributions of this thesis are twofold. The first was the problem formulation, which showed the impracticality of current solutions. The second contribution is the devised framework solution, which is able to resolve the problems inherent in current systems.

6.1.1 Problem Statement

This thesis contributed to the work in the area of network coding. Specifically, a transmission framework for wireless networks employing physical network coding was formulated. As the capacity of networks utilizing single-user strategies decreases as the number of users goes up, the use of physical network coding as a multi-user transmission strategy to increase throughput is promising.

However, current PNC systems relied on several assumptions, chief among which was the synchronization of the received carrier phases of both component signals. We showed that this assumption is untenable, and therefore that the carrier phase offsets between

the two component signals must be considered random. As a result, any demodulation of PNC symbols made up of signals with a rate greater than 1bit/symbol are susceptible to reduced minimum distance and total capacity outage at given carrier offsets.

6.1.2 Proposed Framework Solution

The main contribution of this thesis is a modulation and demodulation solution which is able to provide a reliable decode at any phase offset. The framework solution is able to avoid the problem of symbol ambiguity which affects current systems. Using the observation that binary signalling is not affected by a reduced minimum distance as the carrier phases become asynchronized, a bit-offset modulation and Maximum-Likelihood Sequence Detection framework was devised which can provide systems operating at an arbitrary rate. The following systems were investigated:

- 2 bits/transmission using OQPSK by both sources. The simulated BER curves confirm that this system can operate at any carrier offset.
- 3 bits/transmission using offset 8QAM by the sources. Simulations again shows that the system can operate at any carrier phase offset. This modulation has not been fully designed, however. A phase impulse response will need to be developed for the offset 8QAM such that the resulting modulation possesses bandwidth characteristics that are similar to that of regular 8QAM.

It would seem possible to adapt this system to work with transmissions at arbitrary rates, albeit at the cost of an exponential increase in computation complexity.

6.2 Future Research

There are several promising avenues for future research in the area of physical network coding.

- **Devising specific bit-offset modulation for the PNC framework:** The proposed framework utilizes conventional bit-offset modulation which is probably not optimal for the intended MLSD. As detailed previously, these modulation use a crude instantaneous impulse response. Perhaps a modulation that uses a different impulse response could offer a better decode of PNC signals. Specifically, a decode which is totally invariant to carrier phase offset would be beneficial, as a predictable performance could be obtained in every setting. For the case of offset 8QAM, the phase response is not yet defined. Devising a phase impulse response which allows for the modulation to possess the same bandwidth characteristics as regular 8QAM would validate the use of PNC for transmissions employing 3 bits per symbol.

  As discussed previously, ANC is based on MSK modulation which also employs bit-offset transitions [4]. It would be interesting to consider the MLSD of PNC symbols made up of MSK signals.

  The modulation used for PNC is only constrained to employ binary bit-offset signalling. Thus, as long as the bandwidth budget is respected by the modulation, any bit-offset modulation offering a favourable decode of the resulting PNC symbols could work in our PNC framework.

- **Further characterization of PNC framework:** In this thesis, a heuristic explanation was given for the probability of bit error in the decode of PNC symbols made up of OQPSK. A more thorough characterization could yield models that better predict the performance of PNC systems and provide more insight into the trellis decoding of PNC symbols. This last benefit could in turn assist in the construction of better modulation schemes for the framework. The study of the effects of other asynchrony in the decoding of PNC symbols is also required to better understand

how these systems will fare in a real-life setting. In the initial proposal of PNC, the authors consider carrier frequency and symbol timing asynchrony in addition to carrier phase [3]. The same analysis should be carried out for the proposed framework solution.

- **Study of PNC systems in fading channels:** The wireless media has a random effect on the phase of received signals and is the principal reason that the carrier phases of the component PNC signals cannot be synchronized. In this thesis, we have only considered implicit channel effects on carrier phase. Many practical wireless channels, however, are modelled as having a more complex effect that modifies a signal's amplitude as well as its phase. It would therefore be beneficial to study the proposed framework under these fading channel models.

- **Other ways to demodulate PNC signals:** There are perhaps other ways to compensate for the asynchrony in received PNC signals. For example, a multi-antennae receiver may be able to use its independent channel samples to obtain a satisfactory estimate of both sources' joint information.

Bibliography

[1] R. Ahlswede, N. Cai, S. R. Li, and R. W. Yeung, "Network information flow", in *IEEE Transactions on Information Theory*, IT-46(4), pp.1204-1216, July 2000.

[2] S. Katti, D. Katabi, W. Hu, H. Rahul, and M. Médard, "The importance of being opportunistic: practical network coding for wireless environments", in Proc. 43th Annual Allerton Conference on Communication, Control, and Computing, October 2005.

[3] S. Zhang, S. Liew, and P. Lam, "Physical layer network coding", in *Proc. of ACM MOBICOM*, September 2006.

[4] S. Katti, S. Gollakota, and D. Katabi, "Embracing wireless interference: Analog network coding", in *ACM SIGCOMM*, August 2007.

[5] S. Verdu, *Multiuser Detection*, Cambridge University Press, 1998.

[6] P. Gupta and P.R. Kumar, "The capacity of wireless networks", in *IEEE Trans. Inform. Theory*, 46(2):388-404, March 2000.

[7] P. Gupta and P.R. Kumar, "Towards and information theory of large networks: An achievable rate region", in *Proc. IEEE Int. Symp. Information Theory (ISIT)*, page 150, June 2001.

[8] N. Laneman, D. Tse, and G. Wornell, "Cooperative Diversity in Wireless Networks: Efficient Protocols and Outage Behavior", in *IEEE Transactions on Information Theory*, vol. 50, no. 12, December 2004.

[9] N. Laneman, "Network Coding Gain of Cooperative Diversity", in Proc. IEEE Military Comm. Conf. (MILCOM), November 2004, pp. 106-112.

[10] P. Elias, A. Feinstein, and C. Shannon, "Note on maximum flow through a network", in *IRE Transactions on Information Theory*, IT-2, 117–119, 1956.

[11] S. R. Li, and R. W. Yeung, "Linear Network Coding", in *IEEE Transactions on Information Theory*, IT-49(2), pp.371-381, February 2003.

[12] R. Koetter, M. Médard, "Beyond Routing: An Algebraic Approach to Network Coding", in *IEEE/ACM Transactions on Networking*, vol 11, no 5, October 2003, pp. 782-796.

[13] T Ho, M. Médard, R. Koetter, D R. Karger, M. Effros, J. Shi, B Leong, "A Random Linear Network Coding Approach to Multicast", in *IEEE Transactions on Information Theory*, vol. 52, no. 10, October 2005.

[14] D. Lun, M. Médard, T Ho, R. Koetter, "Network Coding with a Cost Criterion", in *International Symposium on Information Theory and its Applications (ISITA 2004)*, October 2004.

[15] S. Katti, H. Rahul, W. Hu, D. Katabi, M.Médard, J. Crowcroft, "XORs in the air: practical wireless network coding", in *Proc. ACM SIGCOMM*, June 2006

[16] F. Zhao and M. Médard, "On analyzing and improving COPE performance", invited paper, ITA Workshop, 2010.

[17] N. Laneman, D. Tse, and G.Wornell, "Cooperative diversity in wireless networks: Efficient protocols and outage behavior", in *IEEE Transactions on Information Theory*, vol. 50, no. 12, December 2004, pp. 3062 - 3080.

[18] T. Cover, A. El Gamal, "Capacitiy Theorems for the Relay Channel", in *IEEE Transactions on Information Theory*, vol 25, no. 5, September 1979, pp. 572-584.

[19] Y. Wu, P. A. Chou, and S.-Y. Kung, "Information exchange in wireless networks with network coding and physical-layer broadcast", Technical Report MSR-TR-2004-78, 2004.

[20] T. Cover and J. Thomas, *Elements of Information Theory*, New York: Wiley, 1991.

[21] S. Katti, I. Maric, A. Goldsmith, D. Katabi, M. Médard, "Joint Relaying and Network Coding in Wireless Networks", in *IEEE International Symposium on Information Theory*, June 2007, pp. 1101-1105.

[22] I. Maric, A. Goldsmith, M. Médard, "Analog Network Coding in the High SNR Regime", invited paper, ITA Workshop, January 2010.

[23] E. Perrins, R. Schober, M. Rice, M. Simon, "Multiple-Bit Differential Detection of Shaped-Offset QPSK", in *IEEE Transactions on Communications*, vol 55, NO. 12, December 2007.